# The Involvement of Phenylalanine and Phenylacetic Acid in Regulation of Pathogenicity in *B. cenocepacia* K56-2

by

Rebecca Lohmann

A Thesis submitted to the Faculty of Graduate Studies of The University of Manitoba in partial fulfilment of the requirements of the degree of

MASTER OF SCIENCE

Department of Microbiology
University of Manitoba
Winnipeg, Manitoba, Canada

**ABSTRACT**

*Burkholderia cenocepacia* is a gram-negative bacterium known for causing persistent lung infections in individuals living with cystic fibrosis. These infections are highly communicable and difficult to treat due to intrinsic and acquired antibiotic resistance. Previously, our research group found that certain steps in the phenylacetic acid (PAA) degradation pathway are required for full pathogenicity of *B. cenocepacia* in a *Caenorhabditis elegans* host model. Deleting the *paaABCDE* operon, which epoxidizes phenylacetyl coenzyme A (PAA-CoA), causes an attenuation in pathogenicity and abolishes exoprotease activity, a virulence marker, in the presence of phenylalanine. However, deleting the previous step in the pathway, the conversion of PAA to PAA-CoA by the *paaK* ligases, resulted in increased pathogenicity and exoprotease activity. Additionally, deleting *cepR*, a gene involved in quorum sensing, in Δ*paaK* did not abolish exoprotease activity or pathogenicity. I aimed to confirm the phenotype of the Δ*paaK*Δ*cepR* and Δ*paaK* strains and to further characterize the differences in the Δ*paaABCDE* and Δ*paaK* strains in phenylalanine and PAA. I discovered that the Δ*paaK*Δ*cepR* and Δ*paaK* strains likely contain some mutation(s) separate from the PAA degradation pathway that contributes to the presence of pathogenicity. A new Δ*cepR*Δ*paaK* strain has abolished exoprotease activity and attenuated pathogenicity, contradictory to previous results. Additionally, new Δ*paaK* strains have wild-type (WT) levels of exoprotease activity and pathogenicity. Comparing the Δ*paaABCDE* and new Δ*paaK* strains, I found that Δ*paaABCDE* cannot utilize phenylalanine or PAA as a sole carbon source, while Δ*paaK* grows to WT levels on phenylalanine but not PAA. Additionally, Δ*paaABCDE* has abolished exoprotease activity in the presence of these metabolites, while Δ*paaK* has WT levels of exoprotease activity with phenylalanine but significantly decreased levels in the presence of PAA. These same trends were observed in the slow killing assay with *C. elegans* when

the media was supplemented with phenylalanine or PAA. Untargeted metabolomics was used to further investigate these differences but was unsuccessful in elucidating phenylalanine metabolism in the different strains. These results indicate that both phenylacetyl-CoA and phenylacetic acid are involved in the regulation of pathogenicity in *B. cenocepacia* K56-2, but the mechanism is still unknown.

**ACKNOWLEDGEMENTS**

I would like to thank my supervisor, Dr. Silvia Cardona, for providing the space, materials, and guidance for my research along with her support for my future goals. I would also like to thank my committee members, Dr. Karen Brassinga and Dr. John Sorenson, for their support in my research and my thesis. I acknowledge the support provided by NSERC, the Faculty of Graduate Studies, the Faculty of Science, the Graduate Student Association, and the MicroGSA during my studies.

Thank you to all the members of the Cardona lab, past and present, that supported me. They created a welcoming and supportive environment and aided in bringing my spirits up with random songs, videos, and stories. They made the lab feel a little bit like a family. I would also like to thank my family for supporting me from Alberta, despite wishing I had stayed closer. Their support made the distance more bearable. I would like to thank Rayce Funk for being there for me and understanding that sometimes I needed to work late or go in on the weekends even when I'd rather not. Thank you for listening to my presentations and reading my stuff even though you didn't understand most of the 'sciency' words.

And last but not least, I have to thank my cat, Rosa posa. Seeing her waiting for me to come home every day gave me purpose and conviction to finish my degree. I appreciate all the times she ignored my presentations while I practiced and made me stay in bed a little bit longer for cuddles. Her presence in my life made all the bad days a bit more bearable.

**TABLE OF CONTENTS**

## LIST OF TABLES

**LIST OF FIGURES**

## LIST OF ABBREVIATIONS

| | |
|---|---|
| AGC | Automatic Gain Control |
| AHL | Acyl homoserine lactone |
| ANOVA | Analysis of Variance |
| Bcc | *Burkholderia cepacia* complex |
| BCSA | *Burkholderia cepacia* selective agar |
| BDSF | *Burkholderia* diffusible signal factor |
| C6-HSL | *N*-hexanoyl homoserine lactone |
| C8-HSL | *N*-octanoyl homoserine lactone |
| Cci | Cenocepacia island |
| c-di-GMP | Cyclic dimeric guanosine monophosphate |
| CF | Cystic Fibrosis |
| CoA | Coenzyme A |
| DNA | Deoxyribonucleic acid |
| EC | Enzyme Commission number |
| Ep-CoA | Ring 1,2-epoxy-phenylacetyl-CoA |
| Gm | Gentamycin |
| HMDB | Human Metabolome Database |
| Kan | Kanamycin |
| KEGG | Kyoto Encyclopedia of Genes and Genomes |
| LB | Lysogeny broth medium |
| LC-MS | Liquid chromatography mass spectrometry |
| Mb | Megabase |
| NEB | New England Biolabs |
| NGM | Nematode growth medium |
| $OD_{600}$ | Optical density measured at 600 nm |
| *ori* | Origin of replication |
| PAA | Phenylacetic acid |
| PAA-CoA | Phenylacetyl-CoA |
| PBS | Phosphate buffered saline |

| | |
|---|---|
| PCR | Polymerase Chain Reaction |
| Ppm | Parts per million |
| QS | Quorum sensing |
| rDNA | Ribosomal DNA |
| Rha | Rhamnose |
| Rpm | Revolutions per minute |
| RT-qPCR | Quantitative reverse transcription PCR |
| TCA | Tricarboxylic acid |
| Tet | Tetracycline |
| Tp | Trimethoprim |
| WT | Wild type |

# CHAPTER 1: LITERATURE REVIEW

## 1.0 Cystic Fibrosis

Cystic fibrosis (CF) is the most common fatal genetic disease among Caucasians and affects over 100,000 people worldwide. (Blanchard & Waters, 2022; Thornton & Parkins, 2023). CF is an inherited chronic disease that occurs due to defects in the CF transmembrane conductance regulator (Blanchard & Waters, 2022; Lobo & Noone, 2014). This defect results in abnormally thick mucus in the lungs due to impaired mucociliary clearing which provides an excellent environment for microbial colonization (Blanchard & Waters, 2022; Thornton & Parkins, 2023). Common microbes found in the lungs of individuals with CF are opportunistic pathogens that can cause serious infections (Blanchard & Waters, 2022; Lobo & Noone, 2014; Thornton & Parkins, 2023). These infections can result in inflammation and airway obstruction, eventually leading to structural lung and airway damage, and deteriorating respiratory function (Blanchard & Waters, 2022; Thornton & Parkins, 2023). Lung transplantation can be a life-saving operation that prevents fatality from respiratory failure, but infections with certain bacteria can negatively affect the success rate of a lung transplant (Lobo & Noone, 2014; Thornton & Parkins, 2023). Certain strains, such as *Burkholderia cenocepacia*, have been identified as having a negative effect on the success rate of lung transplantation and have been labeled as an absolute contraindication for lung transplantation by many institutions (Lobo & Noone, 2014).

### *1.0.1 Pathogens in CF*

The most prevalent strains found in individuals with CF vary throughout the patient's lifetime. The predominant colonizing species found in infancy and early childhood are

*Haemophilus influenza* and *Staphylococcus aureus* (Lobo & Noone, 2014; Thornton & Parkins, 2023). In adulthood the most predominant species that colonizes CF airways is *Pseudomonas aeruginosa* (Lobo & Noone, 2014; Thornton & Parkins, 2023). However, various other strains have also been found to infect the lungs of individuals living with CF such as *Stenotrophomonas maltophilia, Achromobacter* Spp., *Aspergillus fumigatus*, and various anaerobes (Blanchard & Waters, 2022). One other important group of bacteria to note is the *Burkholderia cepacia* complex (Bcc) which often infects individuals later in life alongside *P. aeruginosa* (Thornton & Parkins, 2023). The Bcc has been used as a marker for progressive lung disease, as increases in prevalence and abundance of these bacteria is often associated with advancing disease severity and accelerated lung function decline (Thornton & Parkins, 2023).

The two most common Bcc strains identified in the lungs of CF patients are *Burkholderia cenocepacia* and *Burkholderia multivorans* (Blanchard & Waters, 2022; Valvano et al., 2005). *B. cenocepacia* was first discovered to be a CF pathogen in the 1980s when it was identified as a highly pathogenic strain with high transmission between patients (Lobo & Noone, 2014). Infection with *B. cenocepacia* carries the greatest risk of morbidity and mortality of all CF-associated organisms (Lobo & Noone, 2014). Additionally, infection with *B. cenocepacia* can lead to cepacia syndrome, a necrotizing pneumonia and septicemia that often leads to death (Lobo & Noone, 2014).

### 1.1 *Burkholderia*

*Burkholderia* was first described as the causative agent of soft rot in onions by W. H. Burkholder in the 1950s (Mahenthiralingam et al., 2005; Valvano et al., 2005; Vial et al., 2011). Originally, this species was labeled as part of the *Pseudomonas* genus, but was later renamed in

the 1990s after its discoverer when it was determined to belong to its own genus (Mahenthiralingam et al., 2005). Since then, over 32 species of *Burkholderia* have been discovered to exist in very diverse ecological niches, ranging from contaminated soils to the respiratory tract of humans (Valvano et al., 2005). *Burkholderia* have been isolated from soils, rhizospheres, water, plants, fungi, animals, hospital environments, and human sources (Vial et al., 2011). These bacteria can exist in such varied ecosystems due to their considerable genetic diversity and metabolic capacity (Mahenthiralingam et al., 2005). Some species have been found to have beneficial interactions with plants as certain species can fix nitrogen and promote plant growth (Eberl & Vandamme, 2016). Other beneficial species have been identified that can degrade pollutants such as toluene and trichloroethylene (Eberl & Vandamme, 2016; Mahenthiralingam et al., 2005). Despite these beneficial properties, some *Burkholderia* species are harmful plant pathogens or opportunistic human pathogens that mainly infect individuals with CF or chronic granulomatous disease (Eberl & Vandamme, 2016; Mahenthiralingam et al., 2005; Valvano et al., 2005; Vial et al., 2011).

### *1.1.1 Burkholderia cepacia complex*

The *Burkholderia cepacia* complex emerged from the *B. cepacia* strain when it was found to consist of at least nine different species with a high degree of 16S rDNA and *recA* similarity (Coenye & Vandamme, 2003). This group is now known to contain over 20 closely related *Burkholderia* species that are very adaptable to changes in their environment (Blanchard & Waters, 2022). The Bcc have large genomes ranging from six to nine megabases (Mb) spread across two to four chromosomes (Mahenthiralingam et al., 2005, Coenye and Vandamme 2003). Additionally, members of the Bcc are intrinsically resistant to most clinically useful antibiotics due to efflux

pumps and chromosomally encoded beta-lactamases (Blanchard & Waters, 2022; Valvano et al., 2005). Members of the Bcc also have a high propensity to acquire antibiotic resistance increasing the difficulty of finding appropriate treatments (Thornton & Parkins, 2023). Multiple virulence factors have been identified in the Bcc bacteria, such as cable pili, type III secretion systems, proteases, biofilm-forming abilities, and quorum sensing systems, which all aid in their ability to cause disease (Blanchard & Waters, 2022; Mahenthiralingam et al., 2005; Valvano et al., 2005). While multiple members of the Bcc are characterized as human pathogens, multiple strains are also commonly found in the plant rhizosphere and are reported as the dominant bacteria in the rhizosphere of rice, pea, or cotton (Vial et al., 2011). Some Bcc strains also release a wide range of antifungals and other compounds that antagonize and repress the growth of many soilborne plant pathogens (Vial et al., 2011).

### *1.1.2 Burkholderia cenocepacia*

*Burkholderia cenocepacia* is a member of the Bcc that has been associated with severe lung disease, increased mortality, and high transmission potential in individuals with CF (Blanchard & Waters, 2022; Thornton & Parkins, 2023). *B. cenocepacia* has a large genome of 8 Mb spread across 3 chromosomes and one large plasmid (Valvano et al., 2005). Infection with *B. cenocepacia* can lead to development of cepacia syndrome, a necrotizing pneumonia with septicemia that is associated with high fatality rates (Blanchard & Waters, 2022; Daccò et al., 2023). Being infected with *B. cenocepacia* can also lead to preclusion from lung transplantation, a life-saving treatment, due to the high risk of reinfection (Blanchard & Waters, 2022; Lobo & Noone, 2014; Thornton & Parkins, 2023). If individuals with a *B. cenocepacia* infection are approved for lung transplantation, the likelihood of death is eight times higher in the first year after

lung transplantation compared to individuals with non-Bcc infections (Alexander et al., 2008). *B. cenocepacia,* and in particular the ET12 epidemic strain, is associated with a fivefold higher mortality compared to other *Burkholderia* strains (Daccò et al., 2023).

### 1.2 Quorum Sensing

Quorum sensing (QS) is a cell-to-cell communication process that bacteria use to communicate and modulate their gene expression in responses to changes in cell density and species composition in their surrounding environment (Abisado et al., 2018; Papenfort & Bassler, 2016; Scoffone et al., 2019). This process is regulated through responses activated by small soluble autoinducer molecules that are produced, secreted, and detected by bacteria (Papenfort & Bassler, 2016; Scoffone et al., 2019). Bacteria monitor their cell numbers through a constitutively expressed autoinducer, and once a threshold level is reached, a cascade of signaling events is triggered leading to expression of hundreds of genes related to bacterial physiology, virulence and biofilm formation (Abisado et al., 2018; Scoffone et al., 2019). QS has been implicated in activating bacterial defense mechanisms such as synchronized production of virulence factors including toxins, proteases, and immune-evasion (Scoffone et al., 2019). Regulation of virulence in human and plant pathogens is often controlled through QS (Bassler, 1999). This regulation aids in a successful infection as bacteria can delay virulence factor production, aiding in evading host immune systems, until a high enough cell number is reached to result in a productive infection (Bassler, 1999).

Gram-negative bacteria use the LuxIR QS system that was first discovered in *Vibrio fischeri* (Bassler, 1999). This system includes LuxI, an autoinducer synthase that synthesizes acyl-homoserine lactone (AHL) autoinducer, and LuxR, the transcriptional activator that binds to the

autoinducer forming a complex that then modulates gene expression by binding to *lux* boxes upstream of target genes (Abisado et al., 2018; Bassler, 1999; Papenfort & Bassler, 2016). LuxR positively regulates the expression of *luxI* resulting in a positive feedback loop (Papenfort & Bassler, 2016). Many bacteria are able to produce and detect multiple different autoinducers, indicating cross-talk between different bacterial species (Papenfort & Bassler, 2016). These AHL QS systems can control diverse behaviours such as production of secreted toxins and virulence factors, biofilm matrix components, and DNA conjugation (Abisado et al., 2018). QS has also been shown to regulate the production of extracellular proteases which aid in infection through providing cells with nutrients by degrading host proteins (Abisado et al., 2018).

### *1.2.1 Quorum sensing in Burkholderia cenocepacia*

The LuxIR QS system is represented by a conserved CepIR system in the Bcc (Gotschlich et al., 2001; Scoffone et al., 2019). CepI mainly synthesizes *N*-octanoyl-homoserine lactone (C8-HSL) and to a minor extent *N*-hexanoyl-homoserine lactone (C6-HSL) (Scoffone et al., 2019). Some *B. cenocepacia* strains also possess a pathogenicity island named cenocepacia island (cci) which contains genes coding for a second AHL-based QS system known as CciIR (Scoffone et al., 2019). In contrast to CepI, CciI mainly produces C6-HSL and lower amounts of C8-HSL (Malott et al., 2005; Scoffone et al., 2019). The CepIR system is the main QS system in the Bcc as members of the Bcc produce approximately ten times more C8-HSL than C6-HSL (Gotschlich et al., 2001). *B. cenocepacia* also has an orphan LuxR homolog, CepR2, whose activation is independent from AHLs but is antagonized by C8-HSL (Scoffone et al., 2019). In the CepIR system, CepR positively regulates the expression of *cepI* and the *cciIR* operon, but negatively regulates its own expression (Scoffone et al., 2019). In contrast, CciR acts as a transcriptional repressor, by negatively

regulating *cepI, cepR2,* and its own expression (Scoffone et al., 2019). It was also found that CepR is required for *cciIR* expression as when *cepR* is deleted, the CciIR system is not active (Malott et al., 2005) The CepIR and CciIR systems have been shown to be non-redundant because *cciI* cannot compensate for mutations in *cepI* and vice versa (Malott et al., 2005).

All Bcc species also contain the *Burkholderia* diffusible signal factor (BDSF) system or cis-2-dodecenoic acid, which is synthesized by $RPfF_{bc}$ and sensed by the soluble receptor RpfR (Scoffone et al., 2019). RpfR is activated by BDSF and degrades cyclic dimeric guanosine monophosphate (c-di-GMP) allowing activation of the global transcriptional regulator GtrR (Scoffone et al., 2019). The BDSF system directly promotes the expression of the AHL synthase genes *cepI* and *cciI* (Scoffone et al., 2019). BDSF binding to RpfR causes a decrease in c-di-GMP which affects swarming motility, biofilm formation, and virulence (Papenfort & Bassler, 2016).

### *1.2.2 Regulation of Virulence Factors through Quorum Sensing*

The quorum sensing system is important for the regulation of virulence factors which is seen when it is disrupted during infection models. The creation of *cepI* or *cepR* mutants in a *B. cenocepacia* H111 strain resulted in an attenuation of virulence in a *Caenorhabditis elegans* host model (Kothe et al., 2003). Additionally, exogenously added C8-HSL led to an increase in the killing ability of the *cepI* mutant, albeit not to wild type (WT) levels (Kothe et al., 2003). Another study showed that a *B. cenocepacia* K56-2 *cepR* mutant did not produce detectable levels of exoprotease, a virulence factor known to be associated with QS (Lewenza et al., 1999). Additionally, interrupting *cepI* resulted in a loss of C8-HSL expression and exoprotease activity, though exogenously adding C8-HSL to the *cepI* mutant was able to restore exoprotease activity (Lewenza et al., 1999). Sokol et al., 2003 also showed that a functional CepIR QS system is

required for full pathogenicity of *B. cenocepacia* in a rat agar bead model. It was shown that strains with mutations in *cepI* or *cepR* had attenuated pathogenicity despite having WT abilities to establish and maintain chronic infections (Sokol et al., 2003). This indicates that the CepIR QS system controls the virulence factors required for a harmful infection in *B. cenocepacia* K56-2 (Sokol et al., 2003). Additionally, it is hypothesized that a zinc metalloprotease gene, *zmpA*, is important in pathogenicity as it was found to be regulated by the CepIR system and may contribute to differences in virulence between CepIR mutants and the parental strain (Sokol et al., 2003).

## 1.3 Phenylacetic acid

Phenylacetic acid (PAA) is a compound found in bacteria, plants, animals, and fungi (Jiao et al., 2022). In plants it is a common auxin that promotes plant growth and plays a role in antimicrobial function, while in fungi it is a direct precursor in the formation of penicillin G and plays a role in metabolism (Jiao et al., 2022). PAA can be toxic at certain concentrations or low pH values and has been shown to disrupt quorum sensing in *P. aeruginosa* (Jiao et al., 2022). PAA is a central intermediate in bacteria that is formed from the degradation of various compounds, such as phenylacetaldehyde, 2-phenylethylamine, and *trans*-styrylacetic acid (Jiao et al., 2022; Luengo et al., 2001). PAA is catabolized through a central route called the PAA degradation pathway, which is the central aromatic compound metabolic pathway that utilizes coenzyme A (CoA), and is present in more than 16% of sequenced bacterial genomes (Jiao et al., 2022; Luengo et al., 2001; Teufel et al., 2010).

### *1.3.1 PAA degradation pathway*

The PAA degradation pathway (Figure 1) is responsible for the conversion of phenylacetic acid to end products; succinyl-CoA and acetyl-CoA (Jiao et al., 2022; Teufel et al., 2010). First,

PAA is converted into phenylacetyl-CoA (PAA-CoA) through the activity of the phenylacetate-CoA ligase, PaaK, which attaches a CoA molecule onto PAA (Jiao et al., 2022; Teufel et al., 2010). PAA-CoA is then epoxidized into ring 1,2-epoxy-phenylacetyl-CoA (ep-CoA) by the activity of the monooxygenase complex PaaABCDE (Teufel et al., 2010). The function of PaaD is currently unknown, but was found to be essential in *E. coli* and may play a role in inducing maturation of the monooxygenase complex (Jiao et al., 2022; Teufel et al., 2010). PaaG then catalyzes a reversible reaction of 1,2-epoxy-phenylacetyl-CoA into 2-oxepin-2(3H)-ylideneacetyl-CoA (Teufel et al., 2010). This compound is acted upon by PaaZ, an oxepin-CoA hydrolase, which forms 3-oxo-5,6-dyhydrosuberyl-CoA (Teufel et al., 2010). Next, PaaJ induces degradation of 3-oxo-5,6-hydrosuberyl-CoA into 3,4-dehydroadipyl-CoA and an acetyl-CoA molecule (Jiao et al., 2022; Teufel et al., 2010). PaaG isomerizes 2,3-dehydroadipyl-CoA, allowing PaaF to form 3-hydroxyadipyl-CoA from the isomerized product (Jiao et al., 2022). PaaH then oxidizes that product to form 3-oxoadipyl-CoA, and finally PaaJ converts 3-oxoadipyl-CoA into succinyl-CoA and acetyl-CoA which can enter into the tricarboxylic acid (TCA) cycle (Jiao et al., 2022; Teufel et al., 2010).

A

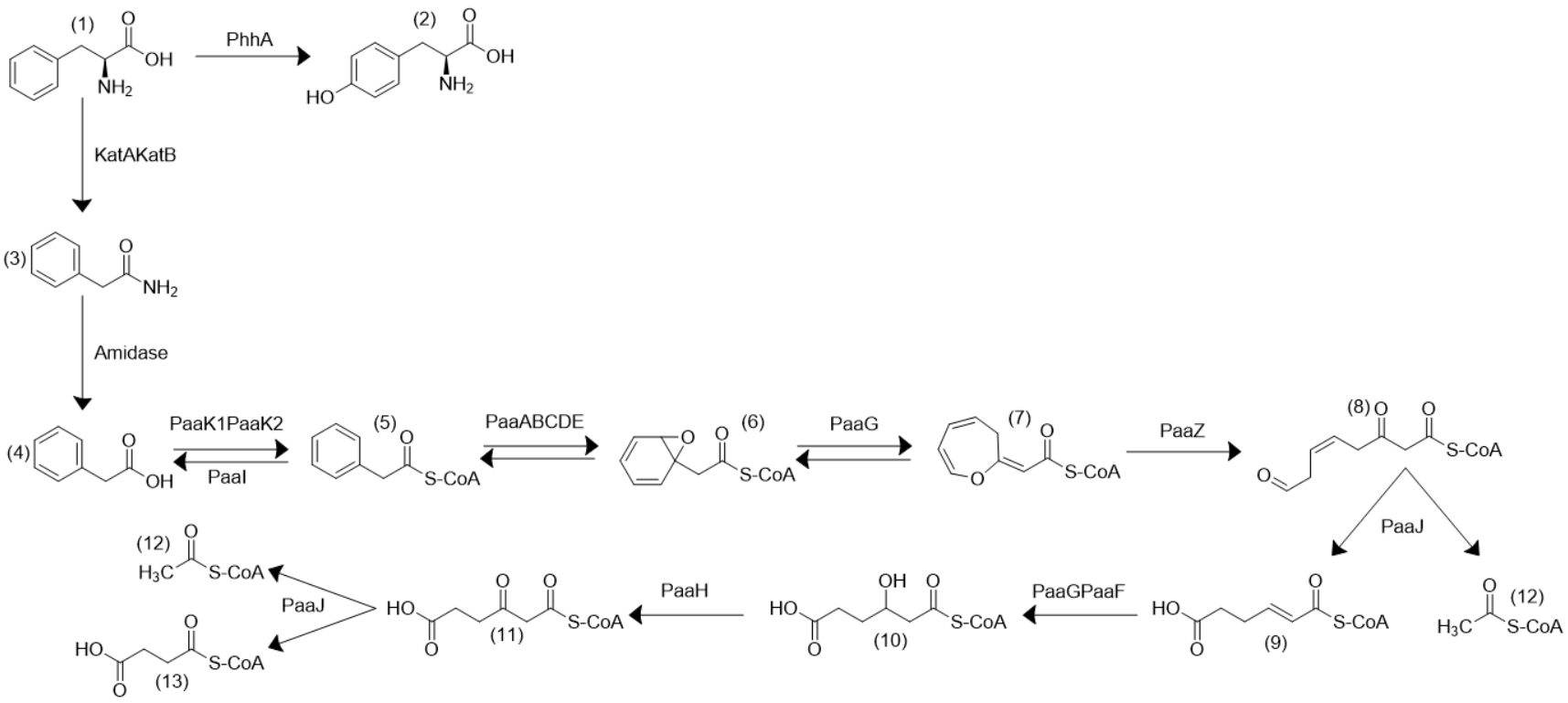
(1)
PhhA
(2)
KatAKatB
(3)
Amidase
(4)
PaaK1PaaK2
PaaI
(5)
PaaABCDE
(6)
PaaG
(7)
PaaZ
(8)
PaaJ
(9)
PaaGPaaF
(10)
PaaH
(11)
PaaJ
(12)
(13)

B

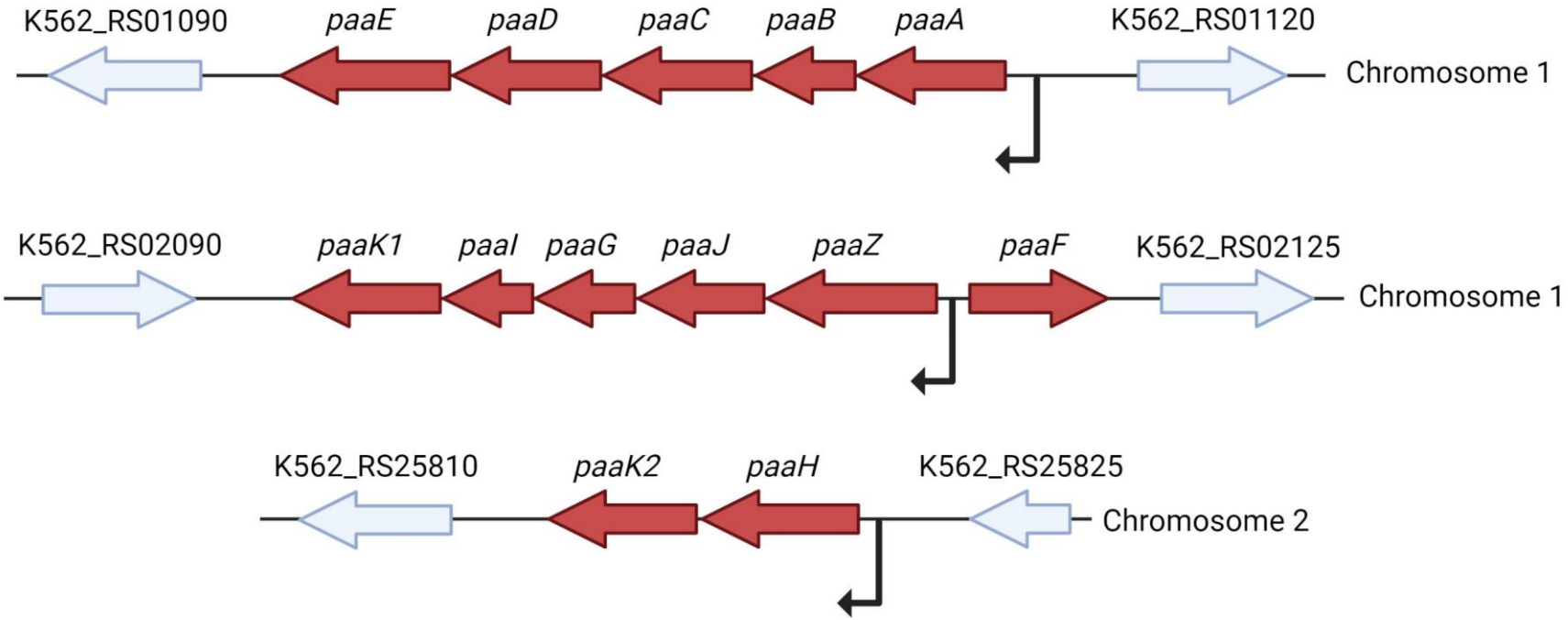


**Figure 1. Phenylalanine degradation pathway in *Burkholderia cenocepacia.***

(A) Shown above is the proposed pathway for phenylalanine degradation in *Burkholderia cenocepacia* as based on studies in *Escherichia coli* and *Pseudomonas* species (Teufel et al., 2010) and annotations from the Kyoto Encyclopedia of Genes and Genomes (KEGG) (Kanehisa, 2019; Kanehisa et al., 2022; Kanehisa & Goto, 2000). Phenylalanine (1) can be converted to tyrosine (2) through the activity of the phenylalanine-4-hydroxylase enzyme, PhhA, subsequent degradation through the tyrosine pathway is not shown. Alternatively, phenylalanine (1) can be converted to 2-phenylacetamide (3) by the catalase peroxidases KatA or KatB, and then phenylacetic acid (PAA) (4) through amidase activity. PAA is then converted to phenylacetyl-coenzyme A (PAA-CoA) (5) by the PaaK1 or PaaK2 ligases, this step can be reversed by the activity of the thioesterase, PaaI. PAA-CoA is then epoxidized to ring-1,2-epoxyphenylacetyl-CoA (6)

by the monooxygenase complex, PaaABCDE, and is then isomerized by PaaG which catalyzes the reversible reaction to 2-oxepin-2(3H)-ylideneacetyl-CoA (7). This compound is acted upon by PaaZ, an oxepin-CoA hydrolase, which forms 3-oxo-5,6-dehydrosuberyl-CoA (8). PaaJ cleaves 3-oxo-5,6-dehydosuberyl into 3,4-dehydroadipyl-CoA (9) and an acetyl-CoA molecule (12). PaaG isomerizes 2,3-dehydroadipyl-CoA, allowing PaaF to form 3-hydroxyadipyl-CoA (10). PaaH then oxidizes that product to form 3-oxoadipyl-CoA (11), and finally PaaJ converts 3-oxoadipyl-CoA into and acetyl-CoA (12) and succinyl-CoA (13). Conversion of phenylalanine to tyrosine or 2-phenylacetamide and further conversion to PAA are deduced based on protein sequence similarity from KEGG, while all steps from PAA downstream are proposed in *B. cenocepacia* from studies done in *E. coli* and *Pseudomonas*. (B) The proposed genetic organization of the PAA catabolic pathway gene clusters in *B. cenocepacia*. The *paaABCDE* and *paaFZJGIK1* operons are located separately on chromosome one while the *paaHK2* operon is located on chromosome two. Regulation of the operons is performed through PaaR binding which prevents transcription, PAA-CoA can cause dissociation of PaaR from the genome. Figure created with BioRender.com.

*1.3.2 Phenylalanine degradation*

In *B. cenocepacia* it is believed that phenylalanine is mainly degraded through the PAA degradation pathway. It has been shown that interruptions in any of the *paaA*, *paaE*, *paaF*, or *paaZ* genes results in a loss of growth in phenylalanine as a sole carbon source (Law et al., 2008; Yudistira et al., 2011) indicating that the PAA degradation pathway is the sole pathway for degradation of phenylalanine in *B. cenocepacia* K56-2. Additionally, phenylalanine was shown to induce the PAA pathway through PAA degradation gene promoter activation (Hamlin et al., 2009) further supporting the hypothesis that this pathway is responsible for phenylalanine degradation. According to the Kyoto Encyclopedia of Genes and Genomes (KEGG) database, *B. cenocepacia* J2315 contains the catalase-peroxidases (Enzyme Commission number (EC):1.11.1.21) required to convert L-phenylalanine into 2-phenylacetamide which can then be converted into PAA through amidase activity (EC:3.5.1.4) (Kanehisa, 2019; Kanehisa et al., 2022; Kanehisa & Goto, 2000). The ability of *B. cenocepacia* K56-2 to grow on 2-phenylacetamide as a sole carbon source has been shown further implying that these steps can convert phenylalanine to PAA in *B. cenocepacia* K56-2 (Yudistira et al., 2011). PAA can then enter the phenylacetic acid degradation pathway described above. However, *B. cenocepacia* is also hypothesized to contain the genes necessary for phenylalanine to enter into the tyrosine degradation pathway through conversion to L-tyrosine by the phenylalanine-4-hydroxylase enzyme (EC:1.14.16.1) (Kanehisa, 2019; Kanehisa et al., 2022; Kanehisa & Goto, 2000). L-tyrosine can be metabolized to 4-hydroxy-phenylpyruvate through the activity of either histidinol-phosphate aminotransferase (EC:2.6.1.9) or aromatic-amino-acid transaminase (EC:2.6.1.57) (Kanehisa, 2019; Kanehisa et al., 2022; Kanehisa & Goto, 2000). 4-hydroxy-phenylpyruvate can then be metabolized by a 4-hydroxyphenylpyruvate dioxygenase (EC:1.13.11.27) into homogentisate which is metabolized through the homogentisate pathway into

acetoacetate and fumarate which can enter into the TCA cycle (Kanehisa, 2019; Kanehisa et al., 2022; Kanehisa & Goto, 2000).

It is possible that the PAA degradation and homogentisate pathways are both active in the degradation of phenylalanine in *B. cenocepacia*. In *Pseudomonas putida*, the degradation of phenylalanine was originally described as proceeding through conversion to tyrosine and subsequent degradation through the homogentisate pathway (Arias-Barrau et al., 2004). However, it was found that *Pseudomonas putida* KT2440 was able to use phenylalanine even if the gene required for conversion to tyrosine was disrupted suggesting a second pathway was present (Herrera & Ramos, 2007). Further analysis revealed that both the conversion of phenylalanine to tyrosine and to PAA was occurring in this strain, revealing that phenylalanine can be degraded by both the homogentisate or PAA degradation pathways in *P. putida* KT2440 (Herrera et al., 2010). While it was shown that *P. putida* KT2440 *paaB* or *paaC* knockout mutants were unable to grow on phenylpyruvate or phenylacetate as sole carbon sources (Herrera et al., 2010), to the best of my knowledge, growth of mutants in the *paaABCDE* operon on phenylalanine has not been tested in this strain.

### *1.3.3 Regulation of the PAA degradation pathway*

The PAA degradation genes in *B. cenocepacia* are organized into three separate operons (Law et al., 2008). Two clusters consisting of the *paaABCDE* operon and the *paaFZJGIK1* operon are located on chromosome one, while the second cluster of *paaHK2* is present on the second chromosome (Law et al., 2008). Despite *paaF* being present on the operon, it is oriented in the opposite direction from the rest of the cluster (Law et al., 2008). The PAA degradation pathway is regulated by two systems, either GntR-type or TetR-type regulators, which both respond to PAA-CoA as an inducer of the pathway (Jiao et al., 2022). The GntR-type regulator is present in *E. coli*

and *Pseudomonas* species, while *B. cenocepacia* has a TetR-type regulator (Jiao et al., 2022). The TetR-type regulator in *B. cenocepacia* was identified and named PaaR by Hamlin et al., 2009 when it was discovered as a negative regulator of the PAA degradation pathway. The *paaR* gene is present downstream of the *paaABCDE* operon but is not in the same transcriptional unit and is transcribed separately (Hamlin et al., 2009). PaaR binds and prevents transcription of the *paaA, paaZ,* and *paaH* operons by binding to their promoter regions (Yudistira et al., 2011). PAA-CoA can bind to PaaR causing it to dissociate from the promoter regions resulting in induction of the pathway (Yudistira et al., 2011). Previously, it was found that PAA does cause an induction of the PAA degradation pathway, likely through conversion to PAA-CoA as PAA does not have a direct effect on PaaR binding (Hamlin et al., 2009; Yudistira et al., 2011). The PAA degradation pathway was also found to be highly upregulated in the CF lung, as *B. cenocepacia* WT K56-2 cells grown in synthetic cystic fibrosis medium had a five-fold increase in the expression of *paaA* (Hamlin et al., 2009; Yoder-Himes et al., 2009). This increase in expression is likely due to the high levels of phenylalanine found in the CF lung sputum (Barth & Pitt, 1996; Palmer et al., 2007)

Bacteria also contain mechanisms to prevent the buildup of toxic compounds such as ep-CoA (Teufel et al., 2012). It has been shown that the *paaABCDE* operon can undo the conversion of PAA-CoA to ep-CoA resulting in a reduction of ep-CoA (Teufel et al., 2012). Additionally, the thioesterase PaaI can undo the conversion of PAA to PAA-CoA, effectively removing excess PAA-CoA (Teufel et al., 2012). The enzymes *paaG* and *paaZ* also function to reduce levels of ep-CoA by converting it into downstream products (Jiao et al., 2022). Together, these mechanisms prevent the buildup of ep-CoA and PAA-CoA aiding in regulation of the pathway (Jiao et al., 2022; Teufel et al., 2012).

*1.3.4 The PAA degradation pathway and virulence*

The PAA degradation pathway has been shown to affect antibiotic resistance and bacterial virulence. It was found that multiple enzymes in the PAA degradation pathway are upregulated in response to meropenem exposure in *B. cenocepacia* (Sass et al., 2011) and multiple steps of the pathway are upregulated in *Acinetobacter baumannii* in response to ciprofloxacin (Kashyap et al., 2021). It has also been shown that high levels of PAA are able to inhibit the pathogenicity of *Rhizoctonia solani* (Jiao et al., 2022). Exogenously adding PAA resulted in a reduction in exoprotease activity and motility in *P. aeruginosa* PAO1 indicating an effect of PAA on the virulence of this strain (Musthafa et a., 2012). Furthermore, addition of PAA to the media resulted in higher survival of *C. elegans* when fed *P. aeruginosa* cultures indicating a reduction in virulence (Musthafa et al., 2012).

Previously in our laboratory, it was found that disrupting the *paaA* or *paaE* genes in the *paaABCDE* operon results in decreased pathogenicity of *B. cenocepacia* K56-2 compared to a WT K56-2 strain in the model organism *C. elegans* (Law et al., 2008). The attenuation of the *paaA* and *paaE* mutant strains was observed 2 days post infection and it was found that complementation was able to fully restore pathogenicity (Law et al., 2008). If the *paaZ* or *paaF* genes, which are present later in the PAA degradation pathway, were interrupted then there was a slight but significant increase in pathogenicity compared to the WT K56-2 strain (Law et al., 2008). In a subsequent study it was found that deleting the *paaABCDE* operon, creating a Δ*paaABCDE* strain, resulted in an attenuated pathogenicity in the *C. elegans* model (Pribytkova et al., 2014). The addition of PAA to the media did not have a significant effect on the killing ability of the WT K56-2 strain, but there was a dose-dependent effect on the Δ*paaABCDE* strain where higher concentrations of exogenously added PAA resulted in further attenuation of the mutant strain

(Pribytkova et al., 2014). This change in pathogenicity was believed to be due to the quorum sensing system in *B. cenocepacia* because a decrease in the *cepI* and *cepR* promoter activity was observed in the Δ*paaABCDE* strain when grown in nematode growth medium (NGM), as seen with a plasmid-based *lux* transcriptional reporter system (Pribytkova et al., 2014). Additionally, the concentrations of AHLs were assessed in the Δ*paaABCDE* and WT strains with a biosensor system from *Agrobacterium tumefaciens* which showed that the WT strain had higher concentrations of AHL in the media compared to the Δ*paaABCDE* strain (Pribytkova et al., 2014). However, only low concentrations of spent media could be used, as higher concentrations inhibited growth (Pribytkova et al., 2014). Additionally, concentrations of PAA greater than 0.3 mM could not be evaluated as they also inhibited growth of the reporter (Pribytkova et al., 2014). Further experiments supported the involvement of the CepIR system in the reduced pathogenicity of the Δ*paaABCDE* mutant as exogenously added C8-HSL caused an increase in pathogenicity of this strain indicating that the attenuation is due to C8-HSL signalling inhibition (Pribytkova et al., 2014). Either PAA or PAA-CoA could be accumulating in the Δ*paaABCDE* strain causing these effects.

To further investigate the role of the PAA degradation pathway in *B. cenocepacia* K56-2 virulence, our laboratory made a mutant in the first step of the pathway, the *paaK* ligase (Lightly et al., 2019). *B. cenocepacia* has two *paaK* genes, thus it was necessary to create a double deletion mutant in both *paaK1* and *paaK2* to observe the effect of a *paaK* deletion (Lightly et al., 2019). When both *paaK* genes are deleted, it was found that this mutant had a higher killing ability on the slow killing assay with *C. elegans* compared to the WT K56-2 strain, and these mutants had higher levels of exoprotease activity than the WT K56-2 strain regardless of the addition of phenylalanine (Lightly et al., 2019). To investigate if these phenotypes were the result of an effect of PAA or

PAA-CoA on the CepIR QS system, a cell-based reporter system was used to investigate the effect of these compounds on CepR:AHL complexes through activation of the *cepI* promoter (Lightly et al., 2019). From this reporter it was shown that neither PAA nor PAA-CoA had a direct result on CepI activity or CepR:C8-HSL formation (Lightly et al., 2019). Additionally, further analysis showed that the transcript levels of *cepI* and *cepR*, as measured by quantitative reverse transcription polymerase chain reaction (RT-qPCR), were not significantly different between the Δ*paaABCDE*, Δ*paaK*, or WT strains (Lightly et al., 2019). This result directly contradicts the previous research which indicated that there was a reduction in *cepI* and *cepR* promoter activity in the Δ*paaABCDE* strain (Pribytkova et al., 2014). The differences in these results could be due to the plasmid-based reporter system used by Pribytkova et al., 2014 since Lightly et al., 2019 used a cell-based reporter system. The results from the plasmid-based reporter system could have been influenced by the presence of PAA, as PAA might have an effect on the copy number of the plasmid or cell metabolism, as seen in *E. coli* (Sobotková et al., 2002). This suggests that an effect on the plasmid-based reporter system from PAA is the cause of the decrease seen in *cepI* and *cepR* promoter activity, and not the deletion of the *paaABCDE* operon. To investigate if the PAA degradation pathway is involved in the CepIR QS system without affecting *cepIR* transcription, *cepR* deletion mutants were created (Lightly et al., 2019). Creating a *cepR* deletion in the Δ*paaK* deletion background resulted in a strain with WT levels of exoprotease activity and virulence, despite a Δ*cepR* mutant being severely attenuated for virulence with abolished exoprotease activity (Lightly et al., 2019). Overall, this suggested the presence of an alternative signalling pathway that can activate virulence in the absence of CepR and PAA-CoA (Lightly et al., 2019).

## 1.4 Research Question

I hypothesized that there is a regulatory element present in *Burkholderia cenocepacia* K56-2 that can activate virulence in the absence of PAA-CoA when the CepIR quorum sensing system is not active. As I will demonstrate in this thesis, I found that the phenylacetic acid degradation pathway is not involved in the activation of virulence in *B. cenocepacia* in the absence of CepR. Furthermore, I found that the phenotypic differences between the Δ*paaABCDE* and Δ*paaK* mutants may be related to the differential metabolism of phenylalanine and PAA as seen by the differences in virulence when these two strains are grown in the presence of the different compounds.

## 1.5 Objectives

The objectives of this work were as follows:

1. To confirm the virulence phenotypes of the previously made Δ*paaK*Δ*cepR* and Δ*paaK* mutants.
2. To remake the Δ*cepR*Δ*paaK* mutant, characterize its phenotype, and complement the *cepR* deletion.
3. To remake the Δ*paaK* mutants, characterize their phenotypes, and complement the *paaK2* deletion.
4. To investigate the differences in the Δ*paaK* and Δ*paaABCDE* mutants in the presence of phenylalanine and phenylacetic acid.
5. To use metabolomics to investigate the metabolic outcomes of phenylalanine and phenylacetic acid in the Δ*paaABCDE* and Δ*paaK* mutant strains.

## 2.0 MATERIALS AND METHODS

### *2.0.1 Strains, Media Preparation and Growth Conditions*

All bacterial strains, listed in Table 1, were grown at 37°C, and liquid cultures were grown with shaking at 230 revolutions per minute (rpm) in lysogeny broth (LB)-Lennox medium (Difco), unless specified otherwise. Plasmids used are listed in Table 2. The following antibiotics were used to select for and maintain plasmids: kanamycin (Thermo Fisher Scientific; 20 μg/mL for *E. coli*), trimethoprim (Sigma-Aldrich; 50 μg/mL for *E. coli*, 100 μg/mL for *B. cenocepacia*), tetracycline (Sigma-Aldrich; 10 μg/mL for *E. coli*, 100 μg/ml for *B. cenocepacia*), and gentamicin (Sigma-Aldrich; 50 μg/mL for *B. cenocepacia*). A stock solution of L-rhamnose (Sigma-Aldrich) was prepared at a concentration of 20% (wt/vol) in deionized water, filter sterilized, and stored at room temperature. Stock solutions of phenylalanine (Sigma-Aldrich) and PAA (Sigma-Aldrich) were prepared at 100 mM in deionized water, filter sterilized, and stored at 4°C, phenylalanine, or room temperature, PAA.

**Table 1. Bacterial strains used in this study.**

| Strain | Description | Reference(s) or Source |
|---|---|---|
| *Burkholderia cenocepacia* K56-2 (LMG18863) (157)[a] | ET12 lineage CF clinical isolate from Toronto | (Darling et al., 1998) |
| *Burkholderia cenocepacia* K56-2 (LMG18863) (676)[a] | Wild-type strain, ET12 clone related to cystic fibrosis clinical isolate J2315 | (Mahenthiralingam et al., 2000) |
| *B. cenocepacia* K56-2 Δ*paaABCDE* | Deletion of *paaABCDE* operon (K562_RS01115-K562_RS01095) in K56-2 #676 | (Pribytkova et al., 2014) |
| *B. cenocepacia* K56-2 Δ*paaK1*Δ*paaK2*(19)[b] | Deletion of *paaK1* (K562_RS02095) and *paaK2* (K562_RS25815) in K56-2 #676 | (Lightly et al., 2019) |
| *B. cenocepacia* K56-2 Δ*paaK1*Δ*paaK2*Δ*cepR*(19)[b] | Deletion of *paaK1* (K562_RS02095), *paaK2* (K562_RS25815), and *cepR* (K562_RS26605) in K56-2 #676 | (Lightly et al., 2019) |
| *B. cenocepacia* K56-2 Δ*cepR*(19)[b] | Deletion of *cepR* (K562_RS26605) in K56-2 #676 | (Lightly et al., 2019) |
| *B. cenocepacia* K56-2 Δ*paaK1*Δ*paaK2*(22)[b] | Deletion of *paaK1* (K562_RS02095) and *paaK2* (K562_RS25815) in K56-2 #676 | This study |
| *B. cenocepacia* K56-2 Δ*paaK2*Δ*paaK1*(22)[b] | Deletion of *paaK2* (K562_RS25815) and *paaK1* (K562_RS02095) in K56-2 #676 | This study |
| *B. cenocepacia* K56-2 Δ*cepR*(22)[b] | Deletion of *cepR* (K562_RS26605) in K56-2 #676 | This study |
| *B. cenocepacia* K56-2 Δ*cepR*Δ*paaK1*Δ*paaK2*(22)[b] | Deletion of *paaK1* (K562_RS02095), and *paaK2* (K562_RS25815) in Δ*cepR*(22) | This study |
| *Escherichia coli* OP50 | Uracil auxotroph | *Caenorhabditis* Genetic Center (CGC, University of |

| | | |
|---|---|---|
| | | Minnesota, Minneapolis, USA) |
| *Escherichia coli* MM290 | F-, φ 80 *lac*ZΔM15 *end*A1 *rec*A1 *hsd*R17 ($r_H^-$, $m_K^+$) *sup*E44 *thi*-1 Δ*gyr*A96 (Δ*lac*ZYA-*arg*F) U169 *rel*A1 | Cardona lab collection |
| *Escherichia coli* DH5α | $F^-$ Φ80*lac*ZΔM15 Δ(*lac*ZYA-*arg*F) U169 *rec*A1 *end*A1 *hsd*R17 ($r_H^-$, $m_K^+$) *pho*A *sup*E44 $\lambda^-$ *thi*-1 *gyr*A96 *rel*A1 | Cardona lab collection |

[a]157 and 676 refer to the stock numbers of these strains in the Cardona lab collection

[b]19 or 22 refer to the years the strains were published or created, respectively, and are added to distinguish between them

**Table 2. Plasmids used in this study.**

| Plasmid | Description[a] | Reference(s) or Source |
|---|---|---|
| pRK2013 | *ori*$_{colE1}$, RK2 derivative, Kan$^R$, *mob*$^+$, *tra*$^+$ | (Figurski & Helinski, 1979) |
| pDAI-SceI-sacB | DHFR promoter controlling e-I-SceI, *sacB*, Tet$^R$ | (Aubert et al., 2014) |
| pDelcepR | pGPI-SceI containing the upstream and downstream regions of *cepR* (K562_RS26605) for marker-less deletion in K56-2 | (Aubert et al., 2013) |
| pDelpaaK1 (pTL17) | pGPI-SceI containing custom gene fragment for the deletion of *paaK1* (K562_RS02095) in K56-2 | (Lightly et al., 2019) |
| pDelpaaK2 (pTL18) | pGPI-SceI containing custom gene fragment for the deletion of *paaK2* (K562_RS25815) in K56-2 | (Lightly et al., 2019) |
| pSCrhaB2 | *ori*$_{pBBR1}$, *rhaR*, *rhaS*, P$_{rhaB}$, Tp$^R$, *mob*$^+$ | (Cardona & Valvano, 2005) |
| pKF2 | pSCrhaB2 expressing rhamnose-inducible *paaK2* (K562_RS25815) | (Lightly et al., 2019) |
| mini-CTX1-rhadCas9 | Tet$^R$ , Ω-FRT-*att*PMCS, *ori*$_{pMB1}$, *int*$_{φCTX}$ , *ori*T, with codon-optimized *dcas9* cloned into *Spe*I and *Not*I sites | (Hogan et al., 2019) |
| mini-CTX1-rhacepR | Mini-CTX1-rhadCas9 with the *dcas9* replaced with *cepR* (K562_RS26605) | This study |

[a]Kan$^R$, kanamycin resistance; Tp$^R$, trimethoprim resistance; Tet$^R$, tetracycline resistance.

*2.0.2 Molecular biology techniques*

Genetic manipulation of *B. cenocepacia* K56-2 was performed via triparental mating with *E. coli* MM290/pRK2013 as a helper strain. Plasmids were maintained in *E. coli* DH5α strains. Polymerase chain reactions (PCRs) were performed with an Eppendorf Mastercycler nexus GSX1 thermocycler or Eppendorf Mastercycler epgradient S thermocycler with either One*Taq* DNA polymerase (New England Biolabs (NEB)), or Q5 High-Fidelity DNA polymerase with high GC buffer (NEB). Primers used are listed in Table 3, and PCR conditions were optimized for each primer pair. Restriction enzymes (NEB) and T4 DNA ligase (NEB) were used as recommended by the manufacturer. Plasmids were isolated using an E.Z.N.A Plasmid DNA Mini Kit (Omega Bio-Tek), PCR product gel extractions were completed with the Monarch DNA Gel Extraction kit (NEB), and PCR products and digested DNA were purified with Monarch PCR & DNA Clean-up kit (NEB).

**Table 3. Primers used in this study.**

| No. | Sequence (restriction sites are underlined) | Template and location[a] |
|---|---|---|
| 153 | GTGGATGACCTTTTGAATGACCTTT | pGPI-SceI, external to MCS |
| 154 | ACAGGAACACTTAACGGCTGACATG | pGPI-SceI, external to MCS |
| 720 | GCCGTAACAGCAGTATTCG | *B. cenocepacia* genome, inside *cepR* (K562_RS26605) |
| 847 | TTCCTGTCAGTAACGAGAAGG | pSCrhaB2, upstream of MCS |
| 848 | CCGCCAGGCAAATTCTGTTT | pSCrhaB2, downstream of MCS |
| 900 | TGCAACTCGTACAACCT | *B. cenocepacia* genome, upstream of *paaK1* (K562_RS02095) |
| 901 | CCTGTGATTTAGGTTCGC | *B. cenocepacia* genome, downstream of *paaK1* (K562_RS02095) |
| 902 | AAGGGCGTGAACTATCC | *B. cenocepacia* genome, upstream of *paaK2* (K562_RS25815) |
| 903 | TAGAACGGCACACCTC | *B. cenocepacia* genome, downstream of *paaK2* (K562_RS25815) |
| 1077 | CCGTGCCATGTTCGACAATC | mini-CTX1-rhacepR, inside of *rhaS* |
| 1080 | GACAAGGGTTCGATCCAG | *B. cenocepacia* genome, upstream of *cepR* (K562_RS26605) |
| 1081 | GATGGCCATCACGTTGCT | *B. cenocepacia* genome, downstream of *cepR* (K562_RS26605) |
| 3127 | CGTATCGCGGCCGCGTTGCGTCAGGGTGCTTC | *B. cenocepacia* genome, 3' end of *cepR* (K562_RS26605) |
| 3128 | TACGCTACTAGTGAATGGAACTGCGCTGGC | *B. cenocepacia* genome, 5' end of *cepR* (K562_RS26605) |

[a]MCS, multiple-cloning site

*2.0.3 Construction of unmarked deletion strains*

Unmarked deletion strains were made with the use of a double homologous recombination method developed by Flannagan et al., 2008. To delete *cepR* (K562_RS26605) in *B. cenocepacia* K56-2, a previously made pDelCepR plasmid from Aubert et al., 2013 containing the DNA sequences flanking *cepR* cloned into the pGPI-SceI plasmid was mated into *B. cenocepacia* K56-2 by tri-parental mating. The pDelCepR plasmid integrates into the genome via homologous recombination. Colonies are picked onto LB medium supplemented with trimethoprim and *Burkholderia cepacia* selective agar (BCSA) without the addition of polymyxin or vancomycin (Henry et al., 1997). Recombination is confirmed with the primer pairs 153+1081 or 154+1080 in colonies that have a dull phenotype on BCSA and are trimethoprim resistant with colony PCR. Next, the pDAI-SceI-sacB plasmid (Aubert et al., 2014), encoding a constitutively expressed I-SceI nuclease, is mated into strains with insertions. This enzyme cuts the I-SceI site on the pDelCepR plasmid in the genome causing a double strand break that triggers DNA recombination resulting in either a parental allele or gene deletion between the flanking sequences. This recombination is selected for by sensitivity to trimethoprim, which would indicate loss of the pDelCepR plasmid from the genome. Deletion of *cepR* is confirmed via colony PCR with primers 1080+1081. Positive clones were cured of the pDAI-SceI-sacB plasmid by growth on LB (no salt) + 20% D-sucrose (Thermo Fisher Scientific) plates due to the inclusion of a *sacB* gene allowing for counterselection of the plasmid. Loss of the plasmid is confirmed by sensitivity to tetracycline. This process can be repeated for double and triple deletion mutants. Deletions of *paaK1* (K562_RS02095) and *paaK2* (K562_RS25815) were made using the pDelpaaK1 and pDelpaaK2 plasmids created by Lightly et al., 2019. The insertion of pDelpaaK1 is confirmed via PCR with primer sets 153+901 and 154+900, while *paaK1* deletion is confirmed with primers 900+901.

Insertion of pDelpaaK2 is confirmed via PCR with primer sets 153+903 and 154+902, while *paaK2* deletion is confirmed with primers 902+903.

*2.0.4 Growth of B. cenocepacia strains on various carbon sources*

Strains of *B. cenocepacia* were grown overnight in two milliliters of LB plus appropriate antibiotics. Two hundred microliters of overnight cultures were washed twice in 1X phosphate buffered saline (Dulbecco's PBS, Sigma-Aldrich) before being resuspended in 1X M9 minimal media (Difco) without a carbon source. The $OD_{600}$ of washed cultures was measured using an Epoch 2 microplate reader (BioTek) and adjusted to an $OD_{600}$ of 0.08 in 1X M9 minimal media. A 100 μL aliquot of cells was added to each well of a clear 96-well plate with 100 μL of the appropriate medium for a starting $OD_{600}$ of 0.04 in triplicate. Final concentrations of 25 mM glucose (Thermo Fisher Scientific), 5 mM phenylalanine, or 5 mM phenylacetic acid were used as carbon sources. Plates were incubated at 37°C with 80% humidity and 230 rpm shaking. $OD_{600}$ point reads were taken at 24 and 48 hours of incubation. Growth assays in nematode growth medium (NGM)II (2.75 g peptone/liter) were performed as described with final concentrations of 2 mM phenylalanine or 2 mM PAA in NGMII.

*2.0.5 Exoprotease Assays*

Strains of *B. cenocepacia* were grown overnight in two milliliters of LB plus appropriate antibiotics. Two hundred microliters of overnight cultures were washed twice in 1X phosphate buffered saline (PBS) before being resuspended in 1X PBS. The $OD_{600}$ of washed culture was measured using an Epoch 2 microplate reader (BioTek) or Synergy 2 microplate reader (BioTek) and adjusted to an $OD_{600}$ of 1.0 in 50 μL of 1X PBS. 3 μL of the $OD_{600}$ corrected culture was

spotted on 2% skim milk (Difco) agar plates, or 2% skim milk agar plates supplemented with either 2 mM phenylalanine or 2 mM PAA in duplicate. Plates were incubated at 37°C with 80% humidity for 48 hrs after which they were imaged using an Alpha Innotech AlphaImager EP (American Laboratory Training) on the epi setting. Zones of clearance were analyzed using ImageJ software and was calculated by subtracting the area of growth of the colony from the area of clearing. Exoprotease assays performed with *paaK2* complemented strains, had 100 μg of trimethoprim added to the 2% skim milk agar plates to maintain the plasmid.

*2.0.6 Slow Killing Assays in Caenorhabditis elegans*

*Caenorhabditis elegans* strain DH26 [*fer-15(b26)II]* was propagated and maintained on NGMI agar (2.5 g peptone/liter) seeded with a lawn of *E. coli* OP50 at 16°C. The DH26 strain was used in this work as it is spermatogenesis defective at 25°C which ensures that the total number of worms does not increase during the slow killing experiment. To collect worms for the slow killing assay, *C. elegans* eggs were harvested by washing the plates with M9 media for worms until 5 mL was collected. A mixture of 5N NaOH (Thermo Fisher Scientific), 10-15% sodium hypochlorite (Sigma-Aldrich), and water was added to the egg mixture which was vortexed intermittently for 3 minutes before being centrifuged at 1500xg for 30 seconds. The supernatant was then removed, and the pellet was washed twice in 1 mL of M9 media for worms. Pellets were concentrated into 100 μL and spotted onto a sterile NGMI plate. Eggs were incubated at 25°C for 1 day to allow for hatching and a halt of growth at L1 stage. L1 stage worms were then washed from the plate using 1-2 mL of M9 media for worms and transferred to NGMI plates spotted with 100 μL of a stationary phase *E. coli* OP50 culture. L1 stage worms were incubated at 25°C for 2 days until they reached L4 stage. In the meantime, bacterial cultures made from an isolated colony were grown overnight

in 2 mL LB at 37°C with 230 rpm shaking. The $OD_{600}$ of overnight cultures were measured and corrected to an $OD_{600}$ of 1.7, of which 50 μL was spread plated on NGMII (2.75 g peptone/liter) plates in duplicate and grown at 37°C overnight. L4 worms were harvested and washed 2-3 times in 500 μL M9 media for worms and then diluted to spot approximately 20-40 worms per NGMII plate. Worms were counted as day 0 and incubated at 25°C for the duration of the experiment. Worms were then counted every 24 hours using a zoom stereoscope (Nikon SMZ 745) for seven days and scored as alive or dead, worms that did not respond to touch with a sterilized needle were classified as dead and removed from the plates.

*2.0.7 paaK2 complementation from a plasmid*

To complement the *paaK* deletion strains, a previously made plasmid, pKF2, containing the *paaK2* gene under rhamnose inducible control was mated into *B. cenocepacia* mutant strains through tri-parental mating (Lightly et al., 2019). This plasmid was made from the backbone of the pSCrhaB2 plasmid, which was used as an empty vector control for *paaK2* complementation experiments. The pKF2 and pSCrhaB2 plasmids were maintained in *B. cenocepacia* by the presence of 100 μg/mL trimethoprim. Presence of the plasmids was confirmed by colony PCR with primer pair 847+848.

*2.0.8 cepR complementation from the genome*

To create mini-CTX1-rhacepR, *cepR* (K562_RS26605) was amplified from genomic *B. cenocepacia* K56-2 DNA using primer pair 3127+3128. The *cepR* PCR fragment and mini-CTX1-rhadCas9 plasmid DNA was digested with restriction enzymes *Spe*I and *Not*I and ran on an agarose gel to confirm size and separate the mini-CTX1-rha backbone from the dCas9 gene. The mini-

CTX1-rha backbone was extracted from the gel and ligated with the digested *cepR* fragment before being transformed into chemically competent *E. coli* DH5α cells. Presence of the plasmid was confirmed through colony PCR with primer pair 720+1077 and mated into *B. cenocepacia* strains with tri-parental mating. The mini-CTX1-rhacepR plasmid is then inserted into the *attB* site of the *B. cenocepacia* genome through homologous recombination.

*2.0.9 Untargeted Metabolomics*

Strains of *B. cenocepacia* were grown in 1X M9 with 25 mM glycerol and with or without the addition of 2 mM $^{13}$C-labeled phenylalanine or 2 mM PAA until an $OD_{600}$ of approximately 1 to 1.5 was reached. An aliquot of culture equivalent to 2 mL with an $OD_{600}$ corrected to 0.6 was centrifuged at 5°C and then washed in 2 mL of phosphate buffer without salt before being centrifuged as before. Cells were then suspended in 1 mL of ice-cold solvent consisting of acetonitrile, methanol, and water in a 2:2:1 ratio and transferred to a 2 mL screw cap tube containing 0.5 mm glass beads (Thermo Fisher Scientific). Samples were then bead-beat using the Bead Mill 24 (Thermo Fisher Scientific) six times at 6.0 m/s for 40 seconds each with 1 minute incubation on ice between each run. Samples were then centrifuged at top speed for 5 minutes at 5°C to pellet debris and the supernatant was transferred to a new Eppendorf tube. This process was repeated with 300 μL and 200 μL of ice-cold solvent with three steps of bead beating each, and the supernatant was pooled for each condition. The supernatant was then flash frozen in liquid nitrogen before being lyophilized with a ModulyoD Freeze Dryer (20 millibar, -50°C) (Thermo Fisher Scientific) overnight. Lyophilized samples were sent to the Biozone Mass Spectrometry Facility in the Chemical Engineering Department at the University of Toronto for liquid-chromatography mass-spectrometry (LC-MS) analysis. Samples were analysed using an Ultimate

3000 UHPLC (Thermo Fisher Scientific) equipped with either a Hypersil Gold C18 column (50 mm x 2.1 mm, 1.9 μm) (Thermo Fisher Scientific) or Acquity BEH HILIC column (3.0 mm x 150 mm, 1.7 μm) (Waters), both equipped with guard columns. The temperature of the column was set to 40°C with a flow rate of 0.4 mL/min. Water and acetonitrile with 0.1% formic acid were used as eluents for the C18 column. The gradient for the C18 column was performed at 5% B for 1 minute, linear gradient to 98% B for 6 minutes, maintained at 98% B for 3 minutes, returned to 5% B over 30 seconds, and finally a re-equilibration at 5% B for 4.5 minutes (total runtime 15 minutes). A solution of 20 mM ammonium acetate and 20 mM ammonium hydroxide in water and acetonitrile were used as solvents for the HILIC column. The gradient for the HILIC column was performed at 50% B for 1 minute, linear gradient to 0% B for 4 minutes, maintained at 0% B for 6.5 minutes, returned to 50% B over 30 seconds, and finally a re-equilibration at 50% B for 3 minutes (total runtime 15 minutes). The autosampler of the Ultimate 3000 UHPLC was loaded with 10 μL liquid samples with an autosampler temperature of 5°C. A Q Exactive Orbitrap mass spectrometer (Thermo Fisher Scientific) equipped with a Heated Electrospray Ionization (HESI II) probe was used for compound detection. The system was operated in negative and positive polarity modes for generating spectra. Full MS spectra were acquired over an *m/z* range from 70 to 1000 with the mass resolution set to 70,000, Automatic Gain Control (AGC) Target of 3e6, max injection time 200 milliseconds, spray voltage 3.5 kV, capillary temperature 320°C, sheath gas 40, aux gas 20, spare gas 5 and s-lens RF level 55. Data-dependent MS2 spectra using a Top10 approach were acquired using a mass resolution of 17,500, AGC Target of 1e5, max injection time 50 milliseconds, isolation window of 0.4 *m/z* and normalized collision energy of 35. After generating the raw peaks, the untargeted metabolomic data was processed and metabolite detection was performed using the Human Metabolome Database (HMDB), KEGG, Biocyc, and mzCloud

databases with a 5 parts per million (ppm) error window using the differential analysis software package Compound Discoverer 3.2 (Thermo Fisher Scientific). Blank cultures without cells were processed as above and included in analysis to remove any background signals that may appear due to the culture or the metabolite extraction process. Additionally, 4-chloro-benzoic acid was included in the solvent as an internal standard.

### *2.0.10 Statistical Analysis*

Statistical analysis for growth assays and exoprotease assays was performed in R 4.2.3 using analysis of variance (ANOVA). The statistical analysis for the slow killing assays was performed in GraphPad Prism 9.4.0 using the Log-rank (Mantel-Cox) test. A p value of 0.05 was used for all statistical tests.

# CHAPTER 3: PAA-COA IS NOT INVOLVED IN CEPIR QUORUM SENSING REGULATED VIRULENCE

## 3.0 Introduction

Previously in the Cardona lab it was found that a Δ*paaK* deletion strain has increased exoprotease activity and virulence compared to the WT K56-2 strain (Lightly et al., 2019). This increase was initially attributed to the CepIR QS system but deleting *cepR* from this strain only reduced the exoprotease activity and virulence back to WT levels, instead of abolishing them (Lightly et al., 2019). These results, together with a prior Δ*paaABCDE* deletion strain having attenuated pathogenicity, indicated a role for PAA-CoA in CepIR QS regulation since PAA-CoA would accumulate in the Δ*paaABCDE* strain but not in the Δ*paaK* strain (Lightly et al., 2019; Pribytkova et al., 2014). However, the exoprotease and pathogenicity phenotypes of these mutant strains, Δ*paaK1*Δ*paaK2*(19) and Δ*paaK1*Δ*paaK2*Δ*cepR*(19) (19 is used to refer to previously published strains), were not complemented to confirm the effect of the *paaK* deletion. Additionally, these strains were made using the double homologous recombination method described above with a pDAI-SceI plasmid that lacked the *sacB* counterselection gene allowing for easy curing of this plasmid (Lightly et al., 2019). Because this plasmid did not have the counterselection gene present, strains were serially sub-cultured approximately 8 times to promote loss of the pDAI-SceI plasmid, a step necessary for subsequent deletions. Due to the many generations required for this curing method, there was a higher chance for spontaneous mutations to arise which could alter the phenotype of the deletion mutants.

I aimed to confirm the effect of the *paaK* deletion on the exoprotease activity of the Δ*paaK1*Δ*paaK2*(19) and Δ*paaK1*Δ*paaK2*Δ*cepR*(19) deletion strains. This was accomplished by

complementing the strains with *paaK2* under a rhamnose inducible promoter and then measuring changes in exoprotease activity due to complementation. A pKF2 plasmid was previously made that contains the *paaK2* gene under rhamnose inducible control which can be used to complement the *paaK* deletion strains (Lightly et al., 2019). It was shown that a Δ*paaK1* deletion mutant can use PAA as a sole carbon source while the double Δ*paaK* deletion strain is unable to grow on PAA as a sole carbon source (Law et al., 2008; Lightly et al., 2019). Thus, complementing the strains with only *paaK2* is sufficient to restore *paaK* ligase activity to the double Δ*paaK* deletion strains. The complemented strains were also tested on the growth assay with PAA as a sole carbon source to confirm that complementation is successful. From these two assays, I can ascertain whether the deletion of the *paaK* genes is solely responsible for the increase in exoprotease activity of the Δ*paaK1*Δ*paaK2*(19) deletion mutant compared to the WT strain, and the presence of exoprotease activity in the Δ*paaK1*Δ*paaK2*Δ*cepR*(19) deletion mutant.

## 3.1 Results

### *3.1.1 Complementation with paaK2 restores growth in PAA to paaK deletion mutants*

Tri-parental mating was used to insert the pKF2 and pSCrhaB2 plasmids into the WT K56-2, Δ*cepR*(19), Δ*paaK1*Δ*paaK2*(19), and Δ*paaK1*Δ*paaK2*Δ*cepR*(19) *B. cenocepacia* strains. The pKF2 plasmid was made from the backbone of pSCrhaB2 (Figure 2), which was used as a negative vector control in all experiments.

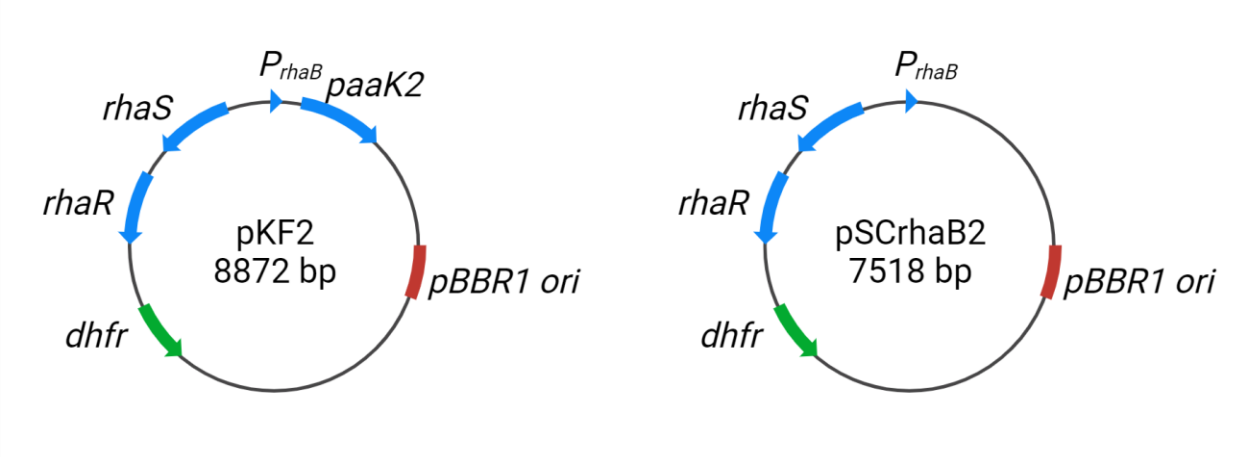


**Figure 2. Plasmid maps of pKF2 and pSCrhaB2 plasmids.**

The pKF2 plasmid was made from the backbone of pSCrhaB2 by inserting the *paaK2* (K562_RS25815) gene cloned from *B. cenocepacia* K56-2 into the plasmid after the $P_{rhaB}$ promoter. Both plasmids have the rhamnose inducible system: *rhaS*, *rhaR*, and the promoter $P_{rhaB}$. The *dhfr* gene confers trimethoprim resistance, allowing for easy selection of the plasmid.

To test whether *paaK2* complementation could restore growth on PAA as a sole carbon source to the Δ*paaK* deletion strains, they were grown in M9 minimal media supplemented with either 50 mM glucose or 5 mM PAA, and with or without 0.01% rhamnose to induce expression of *paaK2*. As shown in Figure 3 all the strains grow similarly in glucose and glucose + rhamnose indicating that the presence of the pKF2 plasmid and the presence of rhamnose does not significantly affect the growth of the strains. Only the WT K56-2 uncomplemented strain harbouring the pSCrhaB2 plasmid had significantly increased growth in glucose or glucose + rhamnose compared to the other strains ($p<0.05$). This is likely because the WT K56-2/pSCrhaB2 strain was made in the *B. cenocepacia* K56-2 (157) background, while all other strains are made in the *B. cenocepacia* K56-2 (676) background. These results convey the importance of using the same background strain for all experiments and exhibits the differences that can be present in the same strains acquired from different sources.

The Δ*paaK1*Δ*paaK2*(19) and Δ*paaK1*Δ*paaK2*Δ*cepR*(19) strains are unable to grow in PAA as a sole carbon source as shown when they are uncomplemented (Figure 3). However, once complemented with *paaK2* and in the presence of rhamnose there is a restoration of growth to approximately WT levels in PAA ($p>0.05$). Overall, this indicates that complementation with *paaK2* is successful in restoring growth in PAA as a sole carbon source to the Δ*paaK* deletion strains indicating that complementation restores the PAA degradation pathway in these strains.

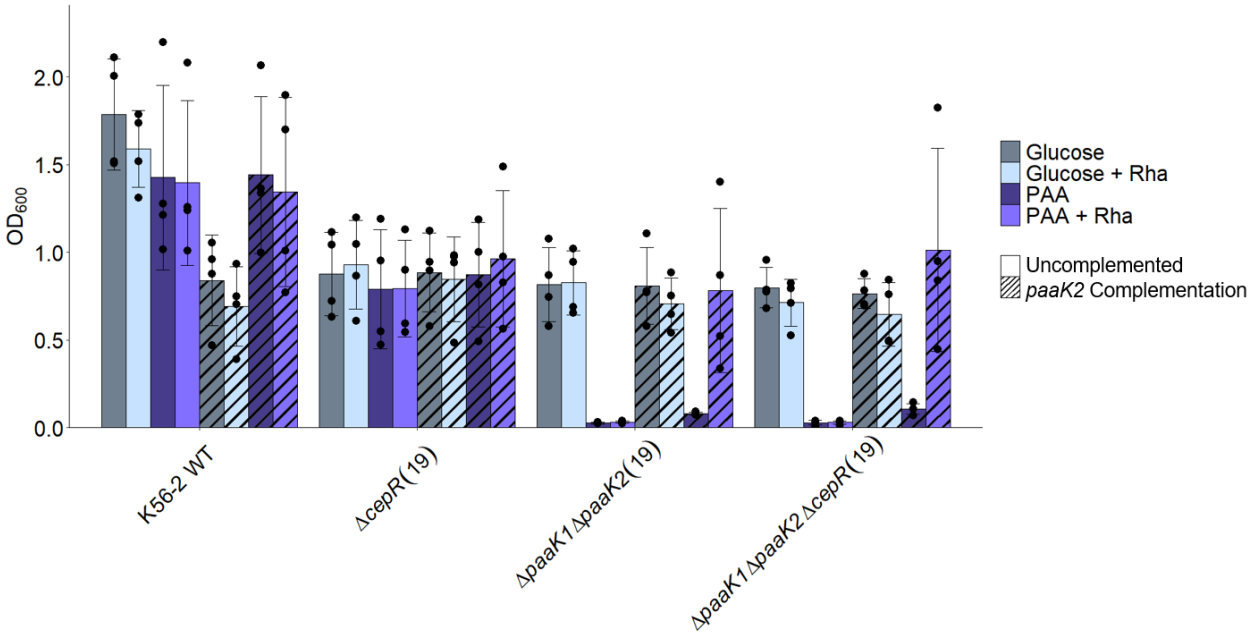


**Figure 3. Complementation of Δ*paaK* deletion strains with *paaK2* restores growth on PAA.**

Overnight cultures of *B. cenocepacia* K56-2 strains with and without *paaK2* complementation were washed twice in 1X PBS before being corrected to an $OD_{600}$ of 0.04. Strains were then grown in 1X M9 minimal media with 25 mM glucose or 5 mM phenylacetic acid (PAA) as a sole carbon source. 0.01% rhamnose (Rha) was added to induce expression of the *paaK2* gene. Optical density readings were taken at 24 hrs. Uncomplemented strains (empty bars) contain the plasmid backbone, pSCrhaB2, without the *paaK2* gene present, while *paaK2* complemented strains (striped bars) contain pKF2. The K56-2 WT uncomplemented strain is from *B. cenocepacia* K56-2 (157), while all other strains are in the *B. cenocepacia* K56-2 (676) background. Error bars are standard deviation of 4 biological replicates performed in triplicate, data points represent the average of each biological replicate.

*3.1.2 paaK2 complementation does not affect exoprotease activity in the ΔpaaK deletion strains*

Since *paaK2* complementation was shown to restore the PAA degradation pathway in the Δ*paaK1*Δ*paaK2*(19) and Δ*paaK1*Δ*paaK2*Δ*cepR*(19) strains, they were next tested on the exoprotease assay to confirm the effect of the *paaK* deletion. Complementing Δ*paaK1*Δ*paaK2*(19) with *paaK2* is expected to result in a decrease in exoprotease levels back to WT, while complementation in Δ*paaK1*Δ*paaK2*Δ*cepR*(19) is expected to abolish exoprotease activity as it would create a practical Δ*cepR* mutant which does not have exoprotease activity. Exoprotease activity of the strains containing the pSCrhaB2 or pKF2 plasmids was assessed on 2% skim milk agar plates with 2 mM phenylalanine and with or without 0.2% rhamnose. As before, strains containing the pSCrhaB2 plasmid were included as a negative control to confirm that the plasmid does not have a significant effect on the exoprotease activity of the strains. Additionally, this control aided in showing that rhamnose does not affect exoprotease activity. Phenylalanine was included in the plates to ensure that the PAA degradation pathway is activated in the strains.

There was a slight decrease in the exoprotease activity of the WT K56-2 strain in the presence of rhamnose in the *paaK2* complementation strain ($p<0.05$), which is likely due to the added energy expenditure of the increased expression of *paaK2* (Figure 4). The Δ*paaK1*Δ*paaK2*(19) uncomplemented strain had significantly less exoprotease activity in the presence of 0.2% rhamnose than without rhamnose or compared to the *paaK2* complemented strain ($p<0.05$). This same trend is seen in the WT K56-2 and Δ*paaK1*Δ*paaK2*Δ*cepR*(19) strains, indicating that there may be a slight effect of the presence of the pSCrhaB2 plasmid on the exoprotease activity of these strains. However, there was no significant difference in the exoprotease activity of the Δ*paaK1*Δ*paaK2*(19) or Δ*paaK1*Δ*paaK2*Δ*cepR*(19) complemented strains with or without rhamnose ($p>0.05$). This indicates that complementation with *paaK2* does

not affect the exoprotease activity of these strains. This is in contradiction to what would be expected if the increase in exoprotease activity and presence of exoprotease activity in the Δ*paaK1*Δ*paaK2*(19) and Δ*paaK1*Δ*paaK2*Δ*cepR*(19) strains, respectively, was due to the deletion of the *paaK* genes in these strains. The Δ*paaK1*Δ*paaK2*Δ*cepR*(19) strain was also found to have significantly lower levels of exoprotease activity in all conditions tested compared to the K56-2 WT strain ($p<0.05$). Previously this strain was reported to have WT levels of exoprotease activity (Lightly et al., 2019), which suggests that the presence of exoprotease activity in this strain is not a stable phenotype.

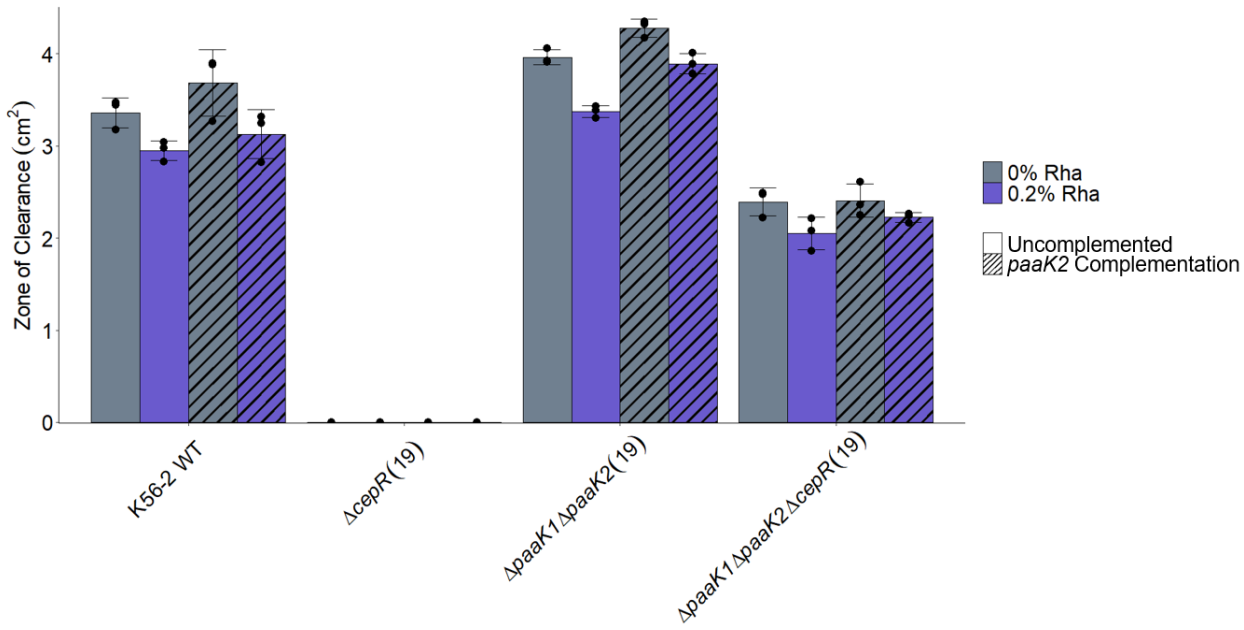


**Figure 4. Complementation with *paaK2* does not affect the exoprotease activity of the Δ*paaK1*Δ*paaK2*Δ*cepR* or Δ*paaK1*Δ*paaK2* mutant strains.**

The exoprotease activity of *B. cenocepacia* strains with or without *paaK2* complementation was quantified by measuring the zone of clearance (excluding colonies) on agar plates containing 2% skim milk and 2 mM phenylalanine with or without the addition of 0.2% rhamnose (Rha) after a 48-hour incubation at 37°C. Rhamnose was added to plates to induce expression of the *paaK2* gene. Uncomplemented strains (empty bars) contain the plasmid backbone, pSCrhaB2, without the *paaK2* gene present, while *paaK2* complemented strains (striped bars) contain pKF2. The K56-2 WT uncomplemented strain is from *B. cenocepacia* K56-2 (157), while all other strains are in the *B. cenocepacia* K56-2 (676) background. Error bars are standard deviation of three biological replicates performed in duplicate, data points represent the average of each biological replicate.

*3.1.3 Creation of new ΔcepR and ΔcepRΔpaaK1ΔpaaK2 strains*

To further confirm that the presence of exoprotease activity in the Δ*paaK1*Δ*paaK2*Δ*cepR*(19) strain was not due to the deletion of the *paaK* genes, I made a new Δ*cepR*Δ*paaK1*Δ*paaK2* deletion mutant in *B. cenocepacia* K56-2. Prior to starting this, I tested two WT K56-2 strains present in the Cardona lab collection and decided to use *B. cenocepacia* K56-2 (676) as this strain has a dull phenotype and shows strong exoprotease activity. Previously the *cepR* deletion was made in a Δ*paaK* deletion background, however, I decided to delete *cepR* (K562_RS26605) first creating Δ*cepR*(22), then subsequently deleting *paaK1* (K562_RS02095) and *paaK2* (K562_RS25815), creating Δ*cepR*Δ*paaK1*Δ*paaK2*(22) (22 is used to refer to newly created strains). This order of deletions should reveal whether a *paaK* deletion can restore virulence to a *cepR* deletion strain. All deletions were confirmed via colony PCR, and the resulting mutant was confirmed to have a dull phenotype on BCSA plates.

First, I characterized the growth of the new Δ*cepR*(22) and Δ*cepR*Δ*paaK1*Δ*paaK2*(22) strains in glucose and PAA as sole carbon sources to confirm that the deletions did not affect their growth and that the PAA degradation pathway is interrupted in the Δ*cepR*Δ*paaK1*Δ*paaK2*(22) strain. As shown in Figure 5 all strains grew similarly in glucose ($p>0.05$), indicating that the deletions did not have a significant effect on growth. Additionally, the Δ*cepR*Δ*paaK1*Δ*paaK2*(22) mutant strain is unable to grow on PAA as a sole carbon source ($p<0.05$) as expected confirming that the PAA degradation pathway is interrupted in this strain.

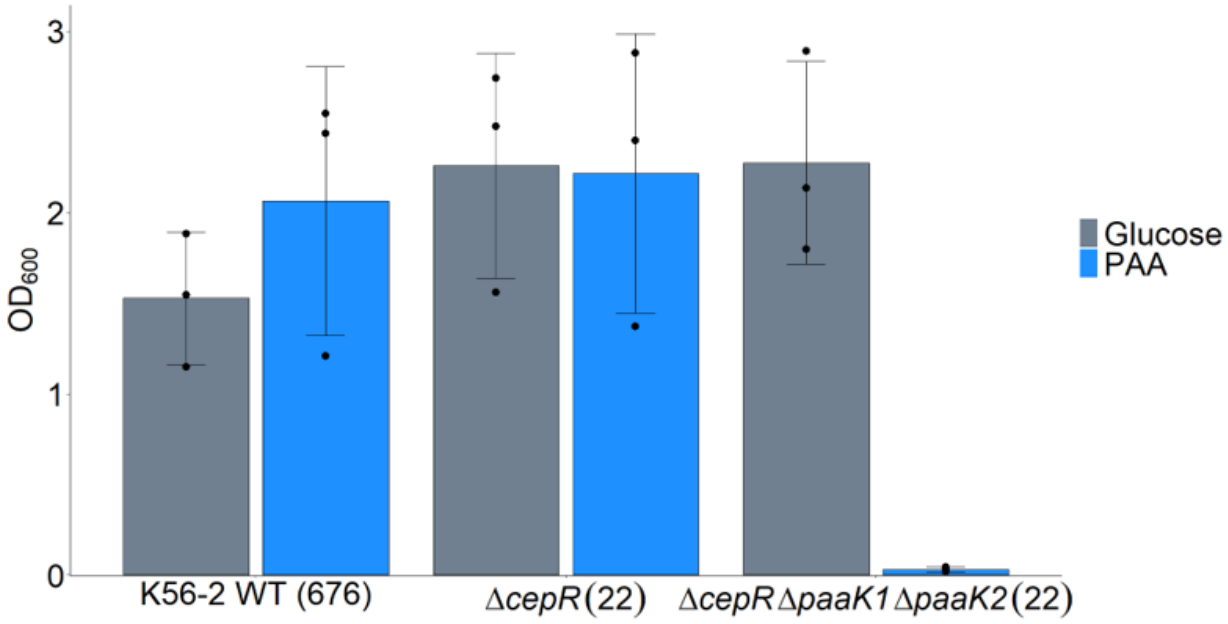


**Figure 5. New Δ*cepR*Δ*paaK1*Δ*paaK2*(22) strain is unable to grow in PAA as a sole carbon source.**

Overnight cultures of *B. cenocepacia* K56-2 mutant strains were washed twice in 1X PBS before being corrected to an $OD_{600}$ of 0.04. Strains were then grown in 1X M9 minimal media with 25 mM glucose or 5 mM phenylacetic acid (PAA) as a sole carbon source. Optical density readings were taken at 24 hrs. Error bars are the standard deviation of three biological replicates performed in triplicate, data points represent the average of each biological replicate.

*3.1.4 The ΔcepRΔpaaK1ΔpaaK2(22) mutant is non-pathogenic*

To assess the exoprotease activity of the Δ*cepR*(22) and Δ*cepR*Δ*paaK1*Δ*paaK2*(22) strains, I grew them on 2% skim milk agar plates with or without 2 mM phenylalanine to induce expression of the PAA degradation pathway. As shown in Figure 6 the Δ*cepR*(22) and Δ*cepR*Δ*paaK1*Δ*paaK2*(22) strains do not produce measurable levels of exoprotease activity after 48 hours of growth regardless of the presence of phenylalanine ($p>0.05$). This contradicts previous results as the Δ*paaK1*Δ*paaK2*Δ*cepR*(19) strains were reported to have WT levels of exoprotease activity after 48 hours of growth (Lightly et al., 2019). This indicates that the Δ*cepR*Δ*paaK1*Δ*paaK2*(22) strain has reduced virulence compared to the WT K56-2 (676) strain, since exoprotease activity is commonly used as a marker of virulence.

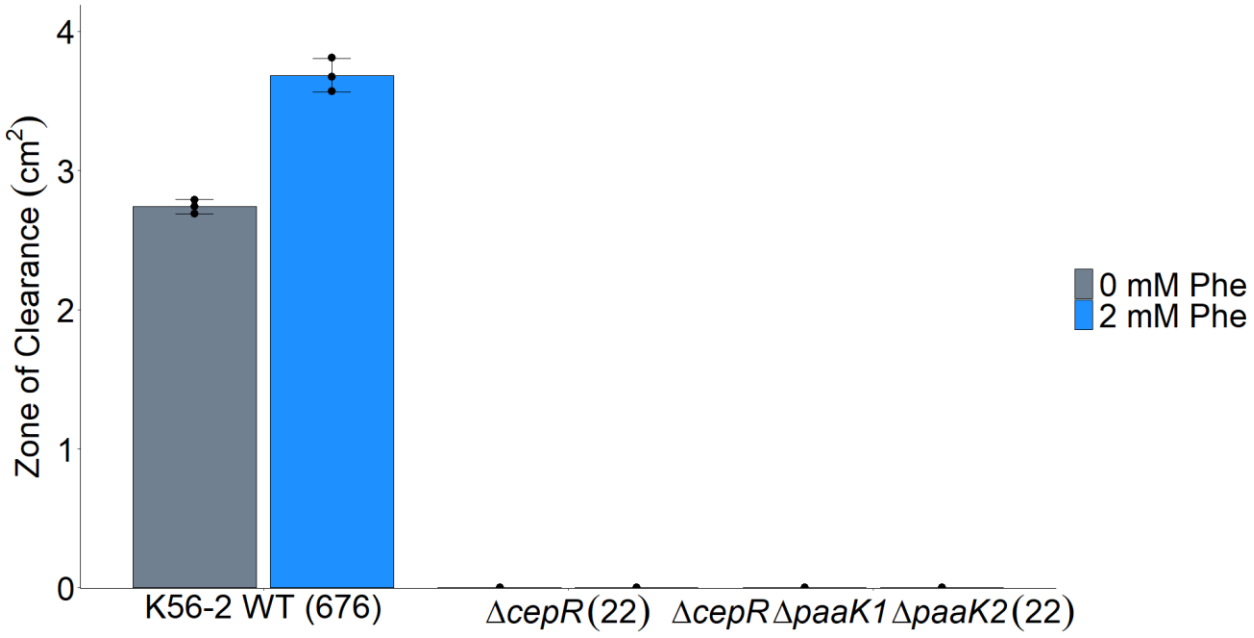


**Figure 6. A new Δ*cepR*Δ*paaK1*Δ*paaK2*(22) deletion strain does not produce exoprotease activity.**

The exoprotease activity of *B. cenocepacia* strains was quantified by measuring the zone of clearance (excluding colonies) on agar plates containing 2% skim milk with or without 2 mM phenylalanine (Phe) after a 48-hour incubation at 37°C. Error bars are standard deviation of 3 biological replicates performed in duplicate, data points represent the average of each biological replicate.

To confirm the virulence of the new Δ*cepR*(22) and Δ*cepR*Δ*paaK1*Δ*paaK2*(22) deletion strains, I tested them on the slow killing assay with *C. elegans*. As shown in Figure 7 the Δ*cepR*(22) and Δ*cepR*Δ*paaK1*Δ*paaK2*(22) strains have similar levels of pathogenicity ($p>0.05$) which is attenuated compared to the WT K56-2 (676) strain ($p<0.05$). *C. elegans* exposed to the WT K56-2 (676) strain show 44% (±11%) survival, while worms exposed to the Δ*cepR*(22) and Δ*cepR*Δ*paaK1*Δ*paaK2*(22) strains show 96% (±2%) and 94% (±5%) survival on day 2, respectively. This is contradictory to previously published results as Δ*paaK1*Δ*paaK2*Δ*cepR*(19) was reported to have the same killing ability as the WT strain (Lightly et al., 2019).

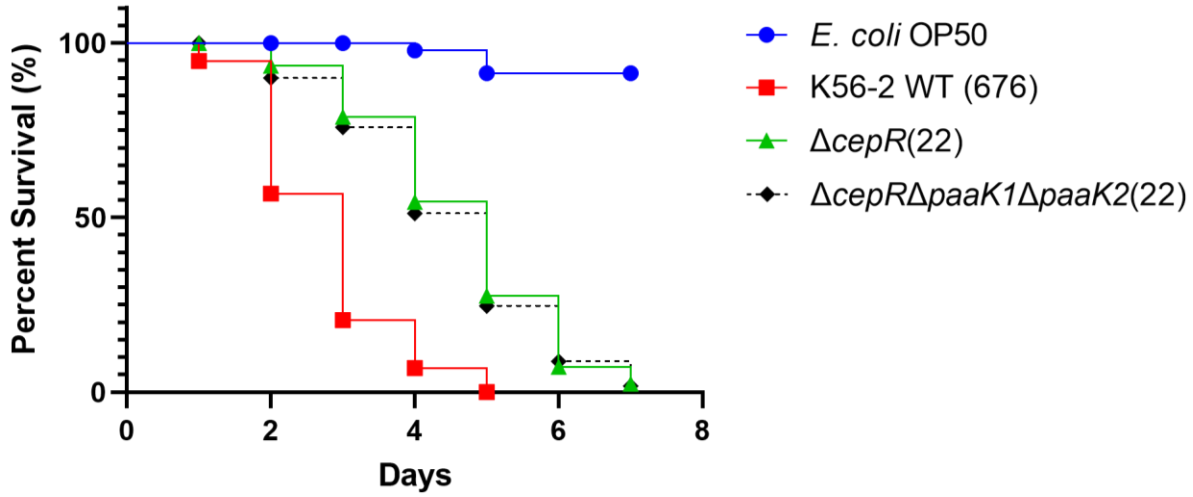


**Figure 7. New Δ*cepR*Δ*paaK1*Δ*paaK2*(22) strain is as attenuated as a Δ*cepR*(22) deletion mutant.**

The pathogenicity of *B. cenocepacia* K56-2 strains was assessed by growing *C. elegans* on NGMII plates seeded with *B. cenocepacia* cultures and assessing their viability over 7 days. The Δ*cepR*(22) and Δ*cepR*Δ*paaK1*Δ*paaK2*(22) strains were not significantly different according to a log-rank test ($p>0.05$). Three biological replicates were performed in duplicate ($n \approx 166$-$357$ worms per strain). Data is plotted in a Kaplan-Meier survival curve and one representative data set is shown.

*3.1.5 Creation of cepR complementation strains*

To confirm that the *cepR* deletion is the sole cause of the abolition of exoprotease activity and pathogenicity in the Δ*cepR*(22) and Δ*cepR*Δ*paaK1*Δ*paaK2*(22) deletion strains, I complemented both strains with *cepR* inserted into the genome under rhamnose inducible control. Complementation was performed with the newly made mini-CTX1-rhacepR plasmid which inserts into the *attB* site of the *B. cenocepacia* K56-2 genome. Presence of the plasmid was confirmed by colony PCR.

*3.1.6 cepR complementation restores pathogenicity to ΔcepR deletion strains*

The exoprotease activity of the *cepR* complemented strains was assessed on 2% skim milk agar plates with or without 0.01% rhamnose to induce expression of the *cepR* gene. As previously shown, without *cepR* complementation both the Δ*cepR*(22) and Δ*cepR*Δ*paaK1*Δ*paaK2*(22) mutant strains lack measurable levels of exoprotease activity after 48 hours (Figure 8). However, when complemented with *cepR* in the presence of rhamnose, there is a significant increase in exoprotease activity compared to the non-complemented conditions ($p<0.05$). Additionally, this increase is to WT levels, complemented for Δ*cepR*(22) and uncomplemented for Δ*cepR*Δ*paaK1*Δ*paaK2*(22), which indicates that only the deletion of *cepR* is responsible for the loss of exoprotease activity in these strains. The presence of the mini-CTX1-rhacepR plasmid in the genome of the WT K56-2 (676) strain appears to confer a slight, but significant, reduction in exoprotease activity ($p<0.05$) in the absence of rhamnose which could be due to the addition of genes in the genome. However, once rhamnose is added to the medium, there is a significant increase in exoprotease activity in the WT K56-2 (676) strain compared to the uncomplemented strain ($p<0.05$). This is likely due to the effect of the CepIR quorum sensing system on exoprotease

activity as it has been previously reported that *cepR* controls exoprotease activity in *B. cenocepacia* (Lewenza et al., 1999; Sokol et al., 2003).

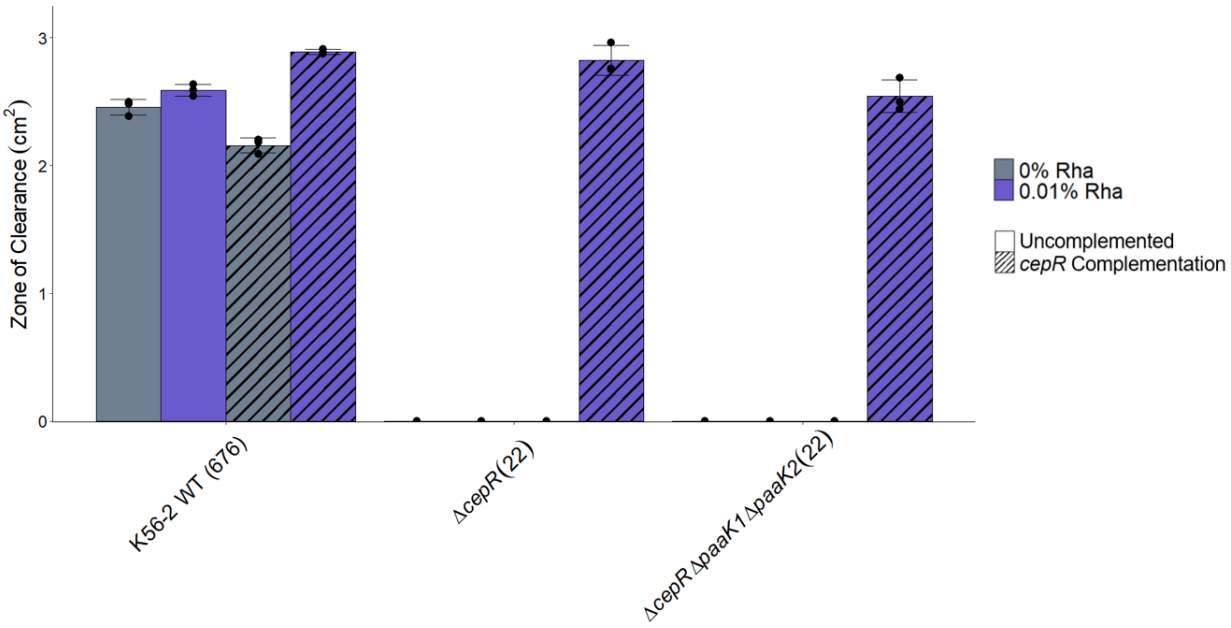


**Figure 8. Complementation with *cepR* restores exoprotease activity to Δ*cepR* deletion mutants.**

The exoprotease activity of *B. cenocepacia* strains with or without *cepR* complementation was quantified by measuring the zone of clearance (excluding colonies) on agar plates containing 2% skim milk with or without the addition of 0.01% rhamnose (Rha) after a 48-hour incubation at 37°C. Rhamnose was added to plates to induce expression of the *cepR* gene. Uncomplemented strains (empty bars) do not contain any insertions, while *cepR* complemented strains (striped bars) have mini-CTX1-rhacepR inserted into the genome. Error bars are the standard deviation of three biological replicates performed in duplicate, data points represent the average of each biological replicate.

Finally, I tested the complemented strains on the *C. elegans* slow killing assay with or without 0.01% rhamnose included in the plates. An *E. coli* OP50 control was used which showed that inclusion of 0.01% rhamnose did not influence the survival of the worms (p>0.05) (

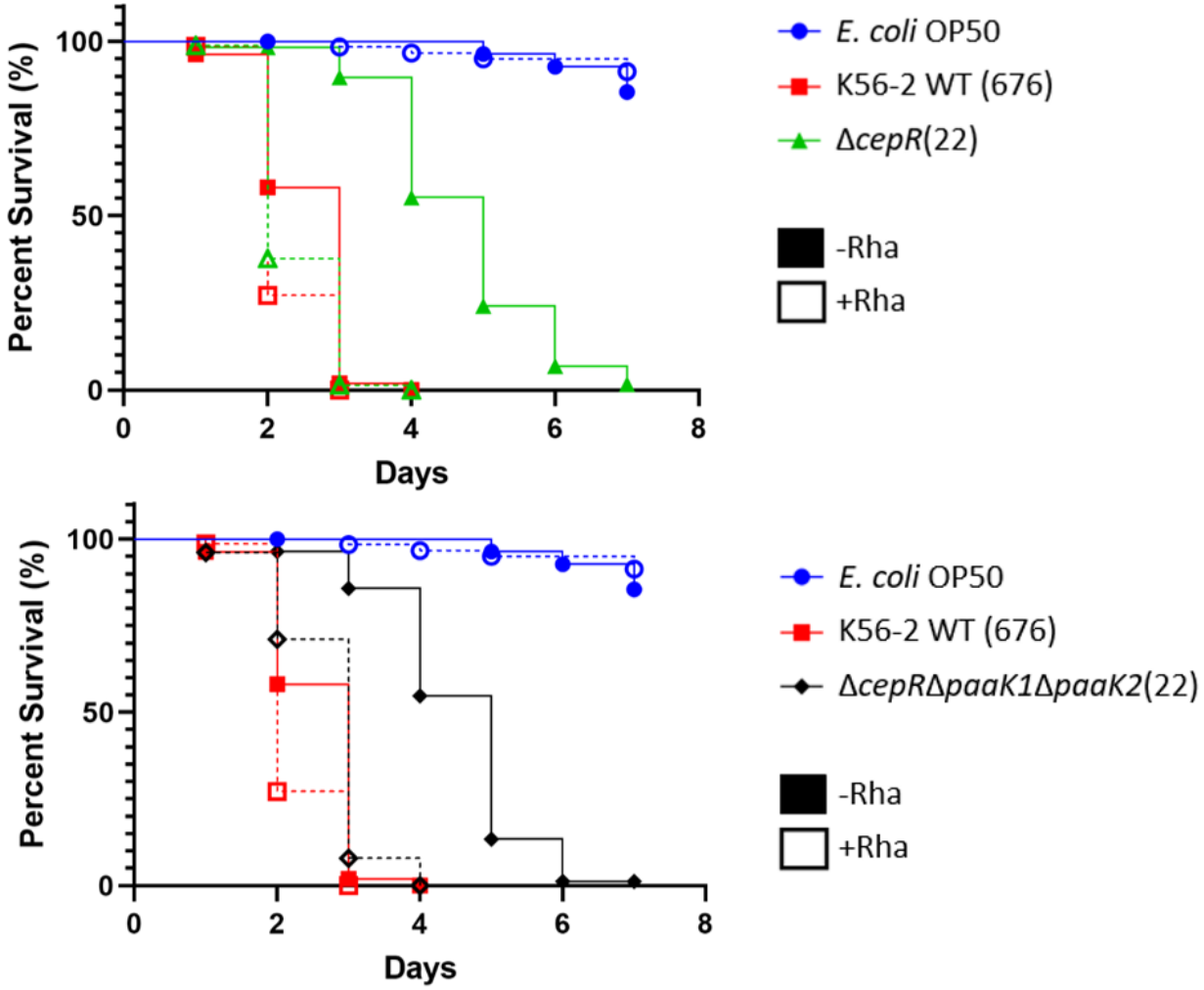


Figure 9). As before, both the Δ*cepR*(22) and Δ*cepR*Δ*paaK1*Δ*paaK2*(22) strains have attenuated pathogenicity as shown by a median survival of 5 days for the *C. elegans*, while worms grown on WT K56-2 (676) have a median survival of 3 days. Once complemented with *cepR* in the presence of rhamnose the Δ*cepR*(22) strain's virulence is increased, which is shown as a median survival of 2 days for *C. elegans* grown on plates with *cepR* complemented Δ*cepR*(22), which is similar to *cepR* complemented WT K56-2 (676) (p=0.005). The *cepR* complemented

Δ*cepR*Δ*paaK1*Δ*paaK2*(22) strain also has increased virulence as shown by a median survival of 3 days for *C. elegans,* which corresponds to uncomplemented WT K56-2 (676) ($p=0.55$). Similar to the exoprotease assay, there was a significant increase in the virulence of the K56-2 WT (676) strain when in the presence of rhamnose ($p<0.0001$). This is attributed to the increased expression of *cepR* because the CepIR QS system has been shown to have an important role in the pathogenicity of *B. cenocepacia* (Kothe et al., 2003; Sokol et al., 2003).

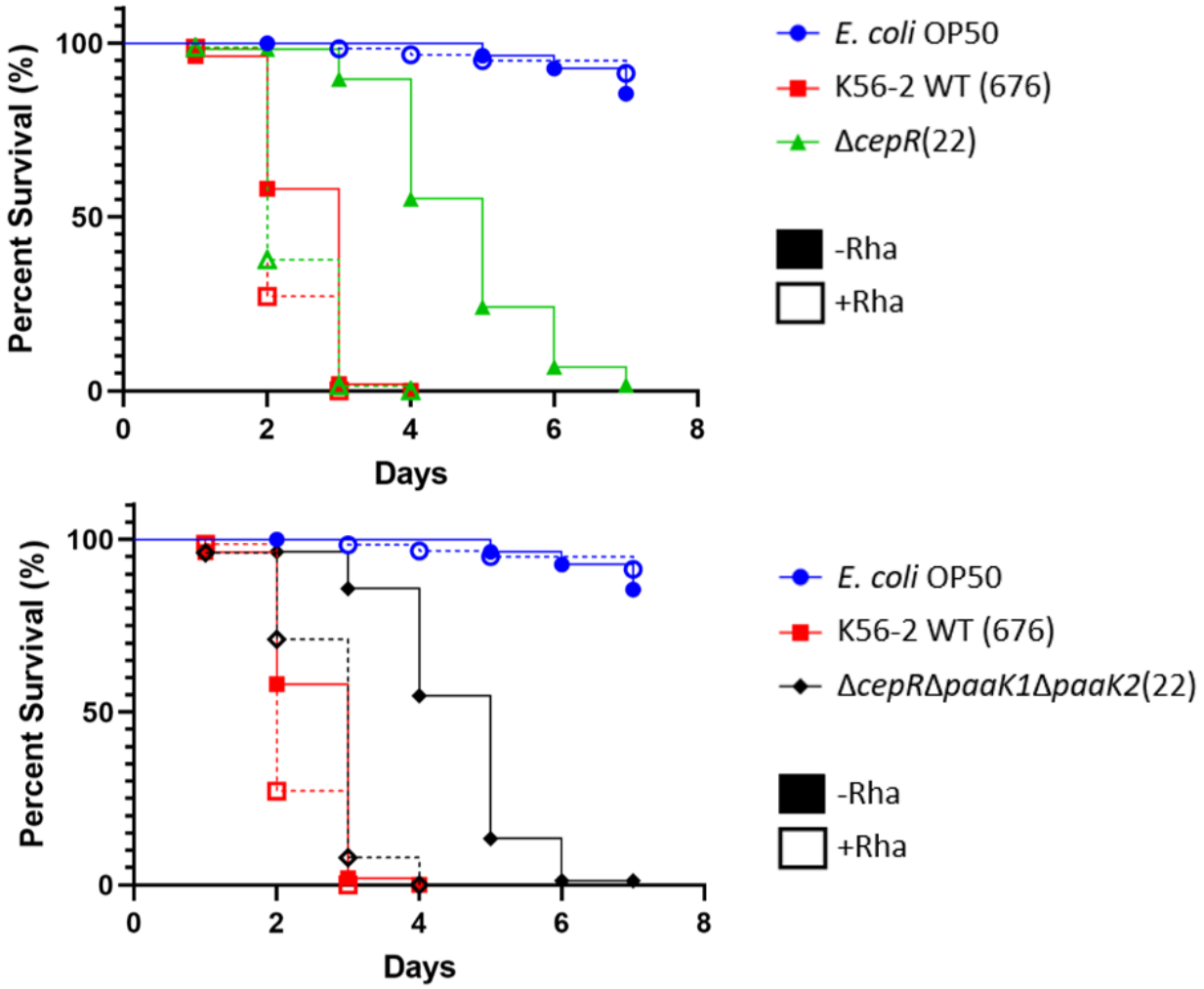


**Figure 9. *cepR* complementation restores pathogenicity to Δ*cepR* deletion mutants.**

The pathogenicity of *B. cenocepacia* K56-2 strains was assessed by growing *C. elegans* on NGMII plates with or without 0.01% rhamnose seeded with *B. cenocepacia* cultures and assessing their viability over 7 days. The *cepR* complemented Δ*cepR*(22) strain's virulence was similar to *cepR* complemented WT K56-2 (676) (p=0.005), while the *cepR* complemented Δ*cepR*Δ*paaK1*Δ*paaK2*(22) strain's virulence was similar to uncomplemented WT K56-2 (676) (p=0.55). Three biological replicates were performed in duplicate (n ≈ 143-206 worms per strain). Data is plotted in a Kaplan-Meier survival curve and one representative data set is shown.

### 3.2 Discussion

Previously it was reported that a *B. cenocepacia* K56-2 Δ*paaK*Δ*cepR* strain had WT levels of exoprotease activity and pathogenicity, which was believed to be influenced by the effect of PAA-CoA on the CepIR QS system (Lightly et al., 2019). Herein I showed through *paaK2* complementation in these strains that there is likely some other mutation acquired during the creation of these strains that influences their virulence. The exoprotease experiment showed that complementation with *paaK2* does not reduce the levels of exoprotease activity in the Δ*paaK1*Δ*paaK2*(19) strain back to WT K56-2 levels or abolish exoprotease activity in the Δ*paaK1*Δ*paaK2*Δ*cepR*(19) strain, as it is abolished in the Δ*cepR*(19) mutant. These lack of changes in exoprotease activity was not due to inadequate complementation as *paaK2* complementation was shown to restore growth on PAA as a sole carbon source indicating restoration of the PAA degradation pathway. Overall, these experiments indicate that the Δ*paaK1*Δ*paaK2*(19) strain contains some acquired mutation that results in an increase in exoprotease activity compared to the WT K56-2 strain. Additionally, since the Δ*paaK1*Δ*paaK2*Δ*cepR*(19) strain was made in the Δ*paaK1*Δ*paaK2*(19) background, this strain likely harbours the same mutation which indicates the presence of exoprotease activity without a functioning quorum sensing system, is not due to the deletion of the *paaK* ligases, but instead is the result of an acquired mutation. Due to the large genome size and genome plasticity (Blanchard & Waters, 2022; Valvano et al., 2005) of *B. cenocepacia* K56-2 and the number of generations used to make these deletion strains, sequencing the strains would likely reveal various mutations. Additionally, it is possible that there is a synergistic effect and not only one acquired mutation that is causing these effects, further decreasing the likelihood that the cause of this increase and presence of exoprotease activity could be found through genome sequencing alone. Due to the

complex regulatory system of pathogenicity in *B. cenocepacia*, which is affected by the activity of at least two separate QS systems and the BDSF system (Scoffone et al., 2019), it would additionally be difficult to determine the effect of any potential mutation found, as it could have a global effect on multiple systems.

The creation of a new Δ*cepR*Δ*paaK1*Δ*paaK2*(22) strain had contradicting results to the previous Δ*paaK1*Δ*paaK2*Δ*cepR*(19) strain despite having the same gene deletions. The new Δ*cepR*Δ*paaK1*Δ*paaK2*(22) strain was found to lack exoprotease activity and have attenuated pathogenicity similarly to the Δ*cepR*(22) strain from which it was made ($p>0.05$). These results indicate that the *paaK* deletion in this strain was not sufficient to restore exoprotease activity or pathogenicity to the Δ*cepR*(22) strain as previously expected. Furthermore, complementation with *cepR* in trans restored exoprotease activity and pathogenicity to both the Δ*cepR*(22) and Δ*cepR*Δ*paaK1*Δ*paaK2*(22) strains to approximately WT K56-2 levels indicating that only the deletion of *cepR* had any effect on these factors.

Overall, these results confirm that there is some other factor at play in the Δ*paaK1*Δ*paaK2*Δ*cepR*(19) strain that is resulting in the presence of exoprotease activity and WT levels of pathogenicity that is not the *paaK* deletion. Also, it is evident from the deletion and subsequent complementation of *cepR* that the CepIR QS system plays a vital role in the pathogenicity of *B. cenocepacia* K56-2. From these results it appears that PAA-CoA does not have a role in CepIR QS regulated virulence, but it is still unclear what role PAA-CoA has on the pathogenicity of *B. cenocepacia* PAA degradation mutant strains. PAA catabolism still has a role in *B. cenocepacia* pathogenicity, though it may not be directly related to QS as previously thought. This is evident by the attenuation of the Δ*paaABCDE* mutant when in the presence of phenylalanine and the lack of attenuation seen in the Δ*paaK* mutant strains. The cause of the

differences between these two mutants in subsequent steps of the PAA degradation pathway are still currently unknown.

# CHAPTER 4: THE PAA DEGRADATION PATHWAY INTERMEDIATES PAA AND PAA-COA PLAY A ROLE IN *B. CENOCEPACIA* PATHOGENICITY

## 4.0 Introduction

The PAA degradation pathway is a well-conserved pathway in bacteria for the metabolism of aromatic compounds (Jiao et al., 2022). However, it may play a role in disease of certain pathogens as PAA degradation pathway genes are upregulated in *B. cenocepacia* during infection in the CF lung (Hamlin et al., 2009; Yoder-Himes et al., 2009). Previously in the Cardona laboratory, it was shown that the *paaABCDE* operon is required for full pathogenicity in the *C. elegans* host model (Law et al., 2008; Pribytkova et al., 2014). However, it was unclear whether an accumulation of PAA-CoA or PAA is responsible for the attenuation of the Δ*paaABCDE* strain as both compounds have the potential to accumulate. Investigation into this hypothesis by deleting the *paaK* ligase genes, the previous step in the pathway, found that a Δ*paaK* deletion mutant had increased pathogenicity (Lightly et al., 2019). This led to the hypothesis that PAA-CoA plays a role in regulation of virulence in *B. cenocepacia* K56-2, but the mechanism was still unclear (Lightly et al., 2019). The increase in pathogenicity of the Δ*paaK* mutants was attributed to a lack of PAA-CoA, while the decrease in the pathogenicity of the Δ*paaABCDE* mutants was attributed to an increase in PAA-CoA, suggesting that PAA-CoA was a negative regulator of virulence traits. It was unclear how PAA-CoA played this role or if PAA had any part in the regulation of *B. cenocepacia* K56-2 virulence.

As shown in Chapter 3, I discovered that the previously made Δ*paaK1*Δ*paaK2*(19) deletion strain likely has an acquired mutation(s) that is responsible for the increase in pathogenicity which may be unrelated to the *paaK* deletions. To elucidate the true phenotype of a Δ*paaK* deletion strain, I remade the Δ*paaK* strains using the double homologous recombination method with the pDAI-

SceI-sacB plasmid containing the *sacB* counterselection gene. I then assessed the new mutants' ability to produce exoprotease and their killing ability in the host model *C. elegans* to ascertain their virulence. Additionally, when testing the new Δ*paaK* deletion mutants, I included the previously made Δ*paaABCDE* deletion strain for comparison as these two mutants are deletions in subsequent steps of the PAA degradation pathway. By comparing these two mutant strains I should be able to determine whether PAA-CoA or PAA is the molecule resulting in the attenuation of pathogenicity observed in the Δ*paaABCDE* mutant strain.

## 4.1 Results

### *4.1.1 Creation of new ΔpaaK mutant strains and phenotypic characterization*

The new Δ*paaK* deletion strains were made in the *B. cenocepacia* K56-2 (676) background strain using the double homologous recombination method developed by Flannagan et al., 2008 by first deleting *paaK1* (K562_RS02095) or *paaK2* (K562_RS25815) and then deleting the second gene to create Δ*paaK1*Δ*paaK2*(22) and Δ*paaK2*Δ*paaK1*(22) deletion mutants (22 is used to refer to newly created strains). The procedure for introducing the deletions was optimized with the pDAI-SceI-sacB plasmid created by Aubert et al., 2014, which allows *sacB* counterselection allowing for rapid curing of the pDAI-SceI-sacB plasmid which is necessary for the second deletion. This optimization eliminated the need for subculturing to remove the second plasmid, which should aid in the reduction of accumulation of secondary site mutations. Presence of the deletions in each strain was confirmed by colony PCR and genome sequencing.

After making the Δ*paaK1*Δ*paaK2*(22) and Δ*paaK2*Δ*paaK1*(22) deletion strains, I tested them on a growth assay with 1X M9 minimal media supplemented with either 25 mM glucose, 2 mM phenylalanine, or 2 mM PAA as sole carbon sources. The WT K56-2 (676),

Δ*paaK1*Δ*paaK2*(22), and Δ*paaK2*Δ*paaK1*(22) strains grew similarly in glucose ($p>0.05$), indicating no effect on growth due to the *paaK* deletions (Figure 10). Interestingly, the Δ*paaABCDE* mutant grew to a significantly higher $OD_{600}$ in glucose than the other strains tested ($p<0.05$), though the reason for this is unknown.

As previously reported, the Δ*paaABCDE* strain is unable to grow on phenylalanine as a sole carbon source. However, it was shown that both the Δ*paaK1*Δ*paaK2*(22) and Δ*paaK2*Δ*paaK1*(22) strains grow to WT levels on phenylalanine ($p>0.05$) (Figure 10). Only the WT K56-2 (676) strain can grow on PAA as a sole carbon source ($p<0.05$), while the Δ*paaABCDE*, Δ*paaK1*Δ*paaK2*(22), and Δ*paaK2*Δ*paaK1*(22) strains are unable to utilize PAA as a sole carbon source. This discrepancy between growth on phenylalanine between the two different mutants is not currently understood, as both mutants have a disrupted PAA degradation pathway. These results suggest that the Δ*paaK1*Δ*paaK2*(22) and Δ*paaK2*Δ*paaK1*(22) strains have a metabolic pathway other than the PAA degradation pathway to metabolize phenylalanine. This pathway could be the homogentisate pathway through conversion of phenylalanine to tyrosine as this pathway has been shown to be used for the degradation of phenylalanine in other strains (Arias-Barrau et al., 2004; Herrera et al., 2010). However, this does not explain the inability of the Δ*paaABCDE* strain to utilize phenylalanine as a sole carbon source. In the Δ*paaABCDE* strain, there is hypothesized to be an accumulation of PAA-CoA since the conversion to ep-CoA is interrupted in this strain. Since PAA-CoA has previously been identified to be a positive regulator of the PAA degradation pathway (Yudistira et al., 2011), the buildup of PAA-CoA in the Δ*paaABCDE* mutant would lead to an overexpression of the PAA degradation pathway genes. This overexpression could result in the sole conversion of phenylalanine to PAA-CoA where further degradation would be inhibited resulting in a lack of growth in this strain. It is also possible

that the regulation of the PAA-CoA genes could be linked to the regulation of alternative phenylalanine degradation pathways such that only one core pathway is upregulated at a time, thus in the Δ*paaABCDE* strain other phenylalanine degradation pathways could be downregulated due to the upregulation of the PAA degradation pathway genes.

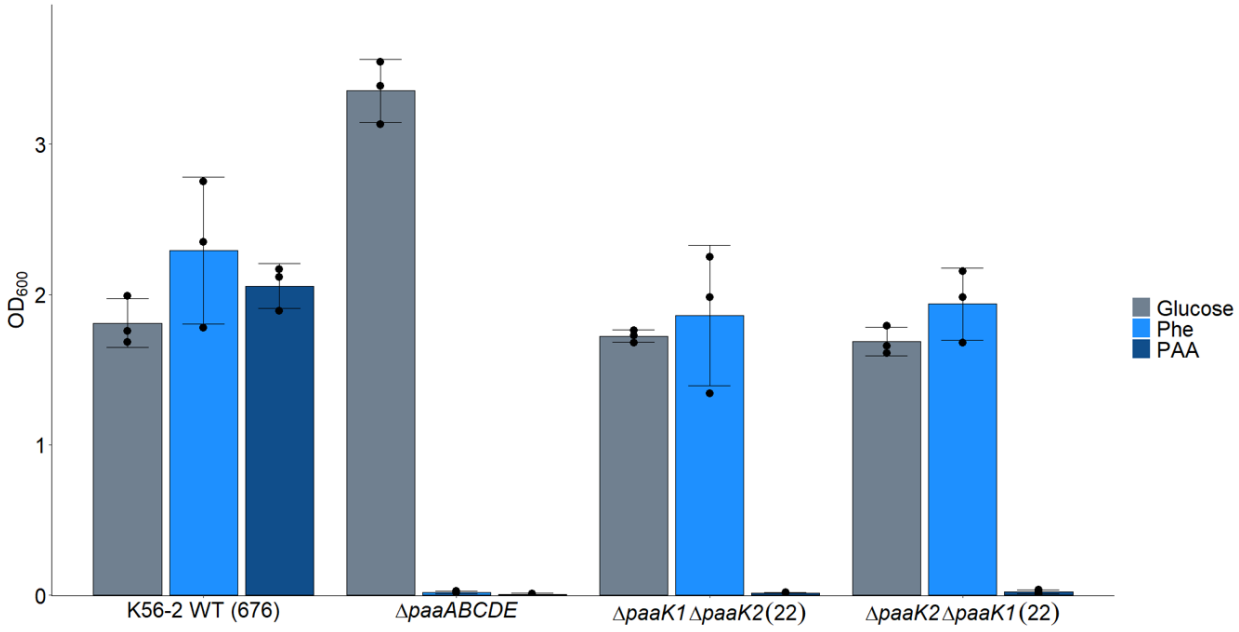


**Figure 10. Δ*paaK* deletion strains can grow on phenylalanine as a sole carbon source, but not on phenylacetic acid.**

Overnight cultures of *B. cenocepacia* K56-2 mutant strains were washed twice in 1X PBS before being corrected to an $OD_{600}$ of 0.04. Strains were then grown in 1X M9 minimal media with 25 mM glucose, 5 mM phenylalanine (Phe), or 5 mM phenylacetic acid (PAA) as a sole carbon source. Optical density readings were taken at 24 hrs. Error bars are the standard deviation of three biological replicates performed in triplicate, data points represent the average of each biological replicate.

Next, I assessed the mutant strains' ability to produce exoprotease on 2% skim milk agar plates that were un-supplemented or supplemented with 2 mM phenylalanine or 2 mM PAA. All strains tested were found to have similar levels of exoprotease activity on the un-supplemented control plate ($p>0.05$) (Figure 11). However, once 2 mM phenylalanine is added to the media, it results in an abolition of exoprotease activity in the Δ*paaABCDE* strain ($p<0.05$), and a significant increase in exoprotease activity of the WT K56-2 (676), Δ*paaK1*Δ*paaK2*(22), and Δ*paaK2*Δ*paaK1*(22) strains compared to the un-supplemented condition ($p<0.05$). Addition of 2 mM PAA to the plates again results in an abolition of exoprotease activity in the Δ*paaABCDE* strain similarly to the addition of 2 mM phenylalanine ($p>0.05$). However, addition of PAA results in a significant decrease in the exoprotease activity of the Δ*paaK1*Δ*paaK2*(22) and Δ*paaK2*Δ*paaK1*(22) strains compared to the un-supplemented and phenylalanine conditions ($p<0.05$). The exoprotease activity of the Δ*paaK1*Δ*paaK2*(22) and Δ*paaK2*Δ*paaK1*(22) strains in the PAA condition is still significantly higher than the Δ*paaABCDE* strain in phenylalanine or PAA ($p<0.05$), but it is significantly decreased compared to the WT K56-2 (676) strain in PAA ($p<0.05$). Addition of PAA does not significantly affect the exoprotease activity of the WT K56-2 strain as compared to the un-supplemented condition ($p>0.05$), indicating that the reduction in the Δ*paaK1*Δ*paaK2*(22) and Δ*paaK2*Δ*paaK1*(22) strains is not solely due to the addition of PAA to the media.

Previously it was reported that the Δ*paaK* deletion strains had increased exoprotease activity compared to the WT K56-2 strain (Lightly et al., 2019). However, in Chapter 3 I discovered that those strains likely contain some acquired mutation(s) that is responsible for the increase in exoprotease activity. I have found that the new Δ*paaK1*Δ*paaK2*(22) and Δ*paaK2*Δ*paaK1*(22) strains have WT levels of exoprotease activity, further confirming the

hypothesis that the previously reported strains contain secondary site mutations that affect their phenotype.

The exoprotease assay results display another phenotypic difference between the Δ*paaABCDE* and Δ*paaK* strains similarly to the difference between these mutants when grown in phenylalanine as a sole carbon source. Interestingly, the exoprotease activity of the strains is only reduced when compounds that they are unable to utilize are added to the media. The absence of exoprotease activity in the Δ*paaABCDE* strain in the presence of phenylalanine or PAA could be influenced by the buildup of PAA-CoA in the media. However, the exoprotease activity of the Δ*paaK1*Δ*paaK2*(22) and Δ*paaK2*Δ*paaK1*(22) strains is only reduced in the presence of PAA, suggesting that PAA may also play a role in *B. cenocepacia* virulence since these strains cannot produce PAA-CoA.

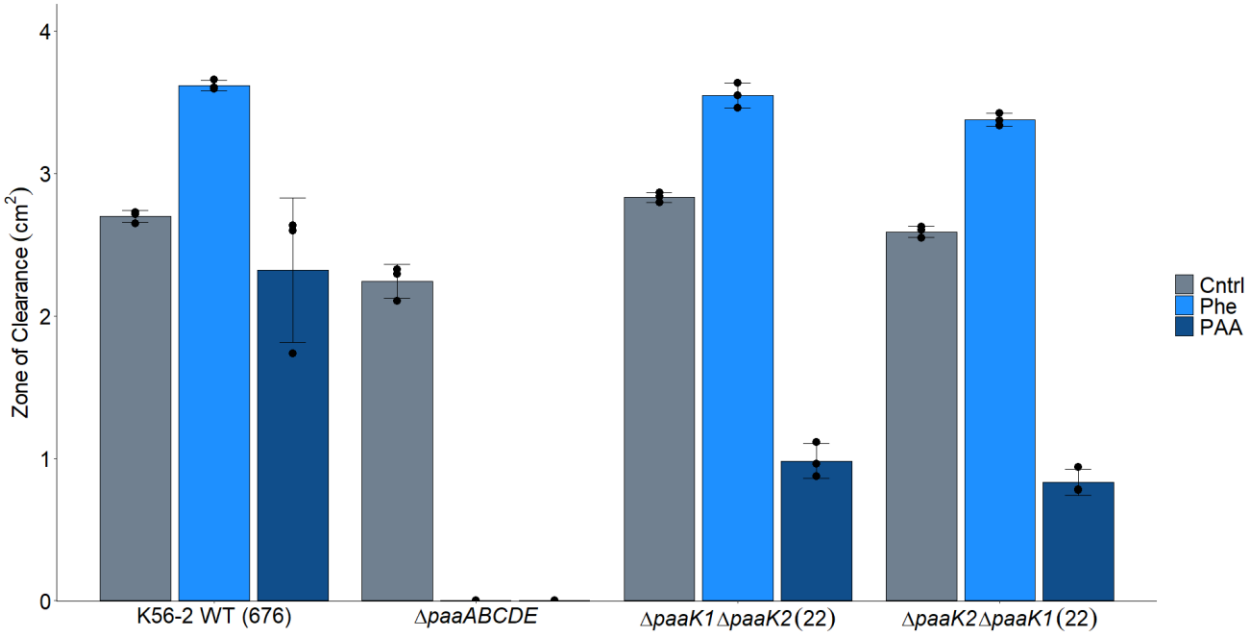


**Figure 11. New Δ*paaK* deletion strains have WT levels of exoprotease activity on phenylalanine, but reduced exoprotease activity on PAA.**

The exoprotease activity of *B. cenocepacia* strains was quantified by measuring the zone of clearance (excluding colonies) on agar plates containing 2% skim milk with or without 2 mM phenylalanine (Phe) or 2 mM phenylacetic acid (PAA) after a 48-hour incubation at 37°C. Control plates (Cntrl) do not contain supplementation. Error bars are the standard deviation of three biological replicates performed in duplicate, data points represent the average of each biological replicate.

After assessing the exoprotease activity of the mutant strains, I determined their pathogenicity on the slow killing assay with *C. elegans*. To determine the effect of the addition of phenylalanine or PAA, 2 mM of either compound was included in the NGMII plates used in this assay. Additionally, an *E. coli* OP50 control was used to confirm that phenylalanine or PAA does not negatively affect the worm's survival. As shown in Figure 12 there was no significant effect on *C. elegans* survival from the inclusion of phenylalanine or PAA in the plates ($p>0.05$). Additionally, the inclusion of phenylalanine or PAA did not affect the killing ability of the WT K56-2 (676) strain, as there was no significant change in the survival of the worms on these plates ($p>0.05$).

As previously reported the Δ*paaABCDE* strain has attenuated pathogenicity compared to the WT K56-2 (676) strain on the control un-supplemented plates ($p<0.05$) (Figure 12). The addition of 2 mM phenylalanine or PAA results in a further attenuation of the Δ*paaABCDE* strain compared to the un-supplemented condition ($p<0.05$). Phenylalanine and PAA resulted in the same attenuation in the Δ*paaABCDE* strain ($p=0.6024$), and worms grown on these plates had similar survival to the *E. coli* OP50 control until approximately day 6 of the assay. These results again correspond to the inability of this strain to utilize phenylalanine or PAA as a sole carbon source, and to the lack of exoprotease activity in the presence of these compounds.

The new Δ*paaK1*Δ*paaK2*(22) and Δ*paaK2*Δ*paaK1*(22) strains have similar levels of pathogenicity as compared to the WT K56-2 (676) strain on the control plates without supplementation ($p>0.05$) (Figure 12). Once 2 mM phenylalanine is added to the plates there is a slight but significant decrease in virulence in both the Δ*paaK1*Δ*paaK2*(22) and Δ*paaK2*Δ*paaK1*(22) strains compared to their killing ability on the un-supplemented plate ($p<0.05$), but this difference is only measurable on day 2 of the assay. The addition of 2 mM PAA

causes a further attenuation in pathogenicity in the Δ*paaK1*Δ*paaK2*(22) and Δ*paaK2*Δ*paaK1*(22) strains ($p<0.05$), which is observed as an approximate one-day shift in the survival curve. These results also indicate a role for PAA in regulation of *B. cenocepacia* pathogenicity as there is no production of PAA-CoA in these strains. However, the role of PAA appears to be minimal compared to the effect of PAA-CoA due to the substantial differences between the effect of the deletion of the *paaK* ligases compared to the deletion of the *paaABCDE* operon.

The Δ*paaK1*Δ*paaK2*(19) strain was previously reported to have increased pathogenicity compared to the WT K56-2 strain (Lightly et al., 2019), however I found that the newly created Δ*paaK1*Δ*paaK2*(22) and Δ*paaK2*Δ*paaK1*(22) strains have WT K56-2 levels of pathogenicity in the *C. elegans* host model. This further supports the hypothesis that the previously made strains contain some mutation(s) that confers an increase in pathogenicity that is unrelated to the *paaK* deletions.

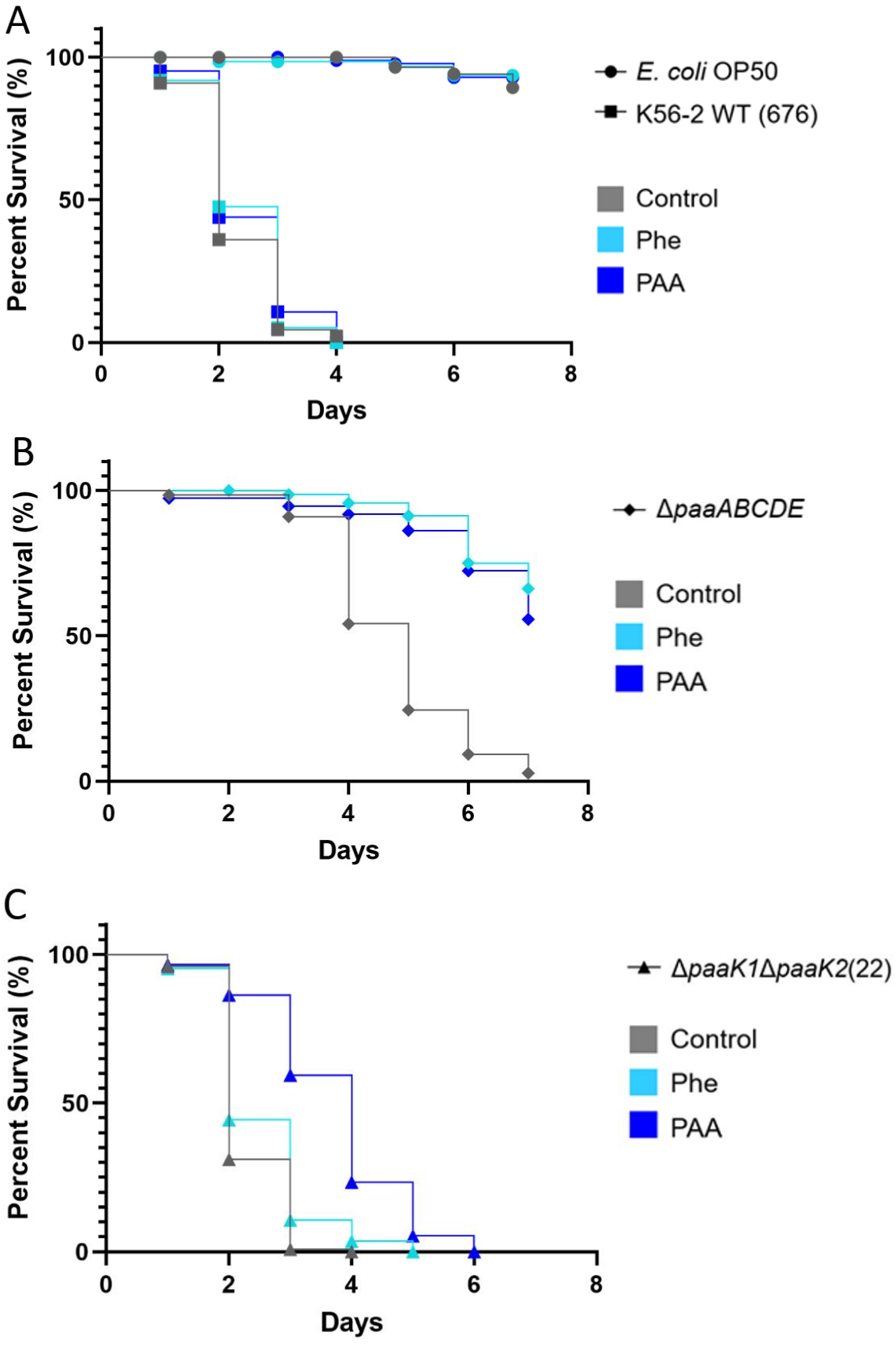
A
Percent Survival (%)
100
50
0
0
2
4
6
8
Days
E. coli OP50
K56-2 WT (676)
Control
Phe
PAA
B
Percent Survival (%)
100
50
0
0
2
4
6
8
Days
ΔpaaABCDE
Control
Phe
PAA
C
Percent Survival (%)
100
50
0
0
2
4
6
8
Days
ΔpaaK1ΔpaaK2(22)
Control
Phe
PAA

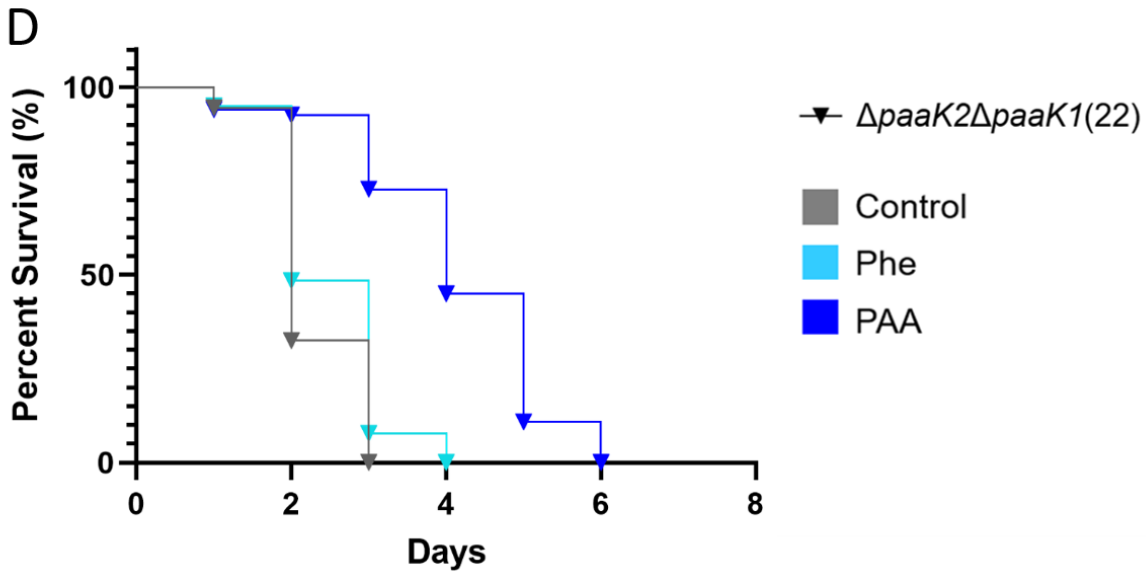


**Figure 12. Δ*paaK* strains have reduced pathogenicity in phenylacetic acid, while Δ*paaABCDE* strains have reduced pathogenicity in phenylacetic acid and phenylalanine.**

The pathogenicity of *B. cenocepacia* K56-2 strains was assessed by growing *C. elegans* on NGMII plates seeded with *B. cenocepacia* cultures and assessing their viability over 7 days. 2 mM phenylalanine (Phe) or 2 mM phenylacetic acid (PAA) is added to the media to assess the effect of these compounds on virulence, un-supplemented plates (control) do not have phenylalanine or PAA added to the plates. (A) Neither the K56-2 WT (676) parental strain nor *E. coli* OP50 were significantly affected by addition of 2 mM phenylalanine or PAA ($p>0.05$). (B) The addition of phenylalanine and PAA resulted in a significant attenuation of the Δ*paaABCDE* strain ($p<0.05$). Both the (C) Δ*paaK1*Δ*paaK2*(22) and (D) Δ*paaK2*Δ*paaK1*(22) strains had significantly different killing abilities on phenylalanine and PAA ($p<0.05$). (A-D) Three biological replicates were performed in duplicate ($n \approx 163$-$301$ worms per strain). Data is plotted in a Kaplan-Meier survival curve and one representative data set is shown.

To verify that the differences in pathogenicity of the strains on the slow killing assay is not due to differences in growth, I evaluated their growth in NGMII liquid media supplemented with either 2 mM phenylalanine or 2 mM PAA. I calculated the growth rate of the strains from the linear portion of the curve and found that all strains have a similar growth rate and that no statistical difference was present between strains in different conditions ($p>0.05$) (Figure 13). I did observe that the WT K56-2 (676) strain grows to a higher final $OD_{600}$ when grown in phenylalanine or PAA compared to un-supplemented NGMII, which is likely due to its ability to utilize these compounds as a carbon source. However, there were no significant changes in pathogenicity of the WT K56-2 (676) strain in the slow killing assay due to the supplementation of phenylalanine or PAA which suggests that higher cell numbers do not influence pathogenicity in this model. Both the Δ*paaK1*Δ*paaK2*(22) and Δ*paaK2*Δ*paaK1*(22) strains had a higher final $OD_{600}$ when grown in 2 mM phenylalanine compared to un-supplemented NGMII or 2 mM PAA. Again, this is likely due to these strains' ability to utilize phenylalanine as a carbon source and did not correspond to a higher killing ability in the *C. elegans* host model. The Δ*paaK1*Δ*paaK2*(22) and Δ*paaK2*Δ*paaK1*(22) strains grew to the same final $OD_{600}$ in un-supplemented NGMII and 2 mM PAA supplemented NGMII, indicating that addition of PAA did not affect the overall number of cells. Additionally, the Δ*paaABCDE* strain had similar final $OD_{600}$ values in all conditions, showing that addition of phenylalanine or PAA does not affect the cell density of this strain. These results show that the addition of phenylalanine or PAA does not have a significant effect on the growth rate of the PAA degradation mutants. Additionally, the decrease in pathogenicity due to the addition of phenylalanine and PAA in the Δ*paaABCDE* strain and due to the addition of PAA in the Δ*paaK1*Δ*paaK2*(22) and Δ*paaK2*Δ*paaK1*(22) strains is not due to a decrease in the growth rate or final density of these strains but is a direct result of a decrease in virulence.

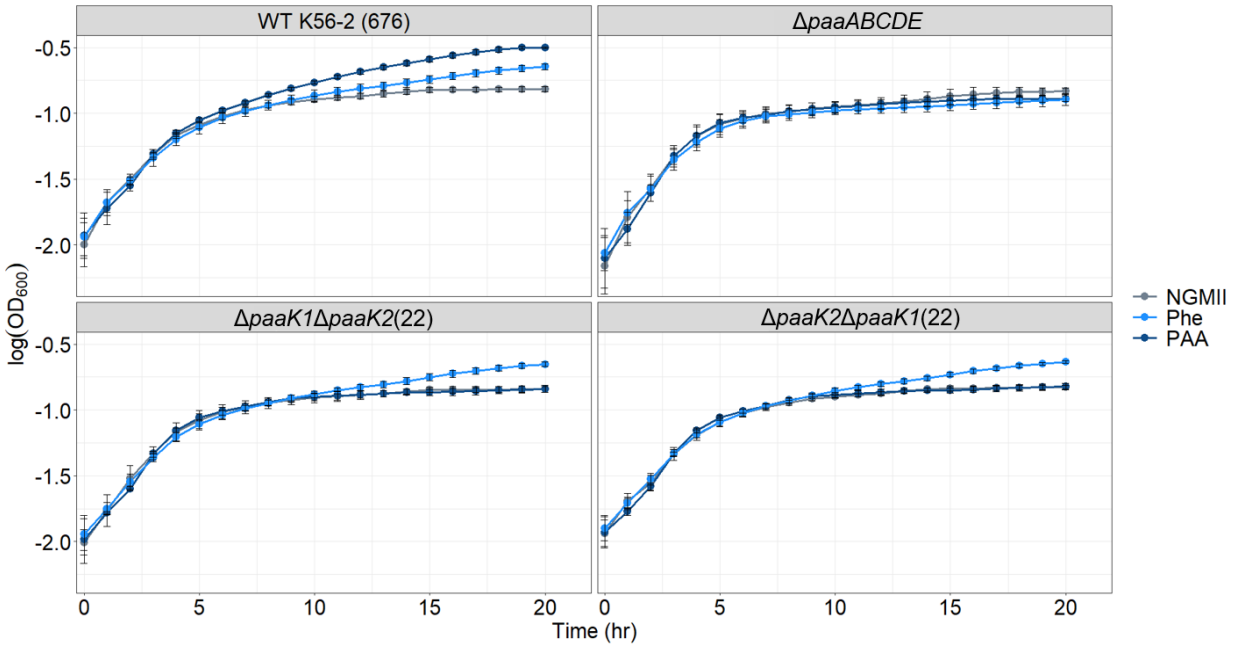


**Figure 13. Addition of phenylalanine or phenylacetic acid does not affect growth rate of PAA degradation mutants.**

Overnight cultures of *B. cenocepacia* K56-2 mutant strains were washed twice in 1X PBS before being corrected to an $OD_{600}$ of 0.04. Strains were then grown in un-supplemented NGMII, or NGMII supplemented with either 2 mM phenylalanine (Phe) or 2 mM phenylacetic acid (PAA). Optical density readings were taken every hour for 20 hours and the $\log_{10}$ values are reported. Error bars are the standard deviation of three biological replicates performed in triplicate. The growth rate was calculated from the first four hours.

*4.1.2 Complementation with paaK2 restores growth and exoprotease activity on PAA*

To confirm the effect of the *paaK* deletions on the growth and exoprotease activity in PAA of the new Δ*paaK1*Δ*paaK2*(22) and Δ*paaK2*Δ*paaK1*(22) deletion strains I complemented them with *paaK2* using the pKF2 plasmid. This plasmid contains the *paaK2* gene under rhamnose inducible control and a trimethoprim resistance gene as a selection marker. The pSCrhaB2 plasmid was included as a control as it is the backbone from which the pKF2 plasmid was constructed. Both plasmids were mated into the *B. cenocepacia* K56-2 strains, and their presence was confirmed via colony PCR.

First, I assayed the growth of the complemented strains in PAA as a sole carbon source. All strains tested grew similarly in glucose and glucose + rhamnose conditions regardless of complementation ($p>0.05$), indicating that the presence of the pKF2 plasmid or the expression of *paaK2* does not have a significant effect on overall growth (Figure 14). Additionally, all conditions of the WT K56-2 (676) strain had similar growth in PAA regardless of the presence of the pKF2 plasmid or rhamnose ($p>0.05$), which indicates that presence of the plasmid or rhamnose does not significantly affect growth. As shown before, neither Δ*paaK1*Δ*paaK2*(22) nor Δ*paaK2*Δ*paaK1*(22) can grow on PAA as a sole carbon source without *paaK* complementation. However, once complemented with *paaK2* and in the presence of rhamnose both strains' growth is restored in PAA to similar levels as the WT K56-2 (676) strain ($p>0.05$). These results show that complementation is successful in these strains at restoring *paaK* ligase activity and therefore restoring the PAA degradation pathway.

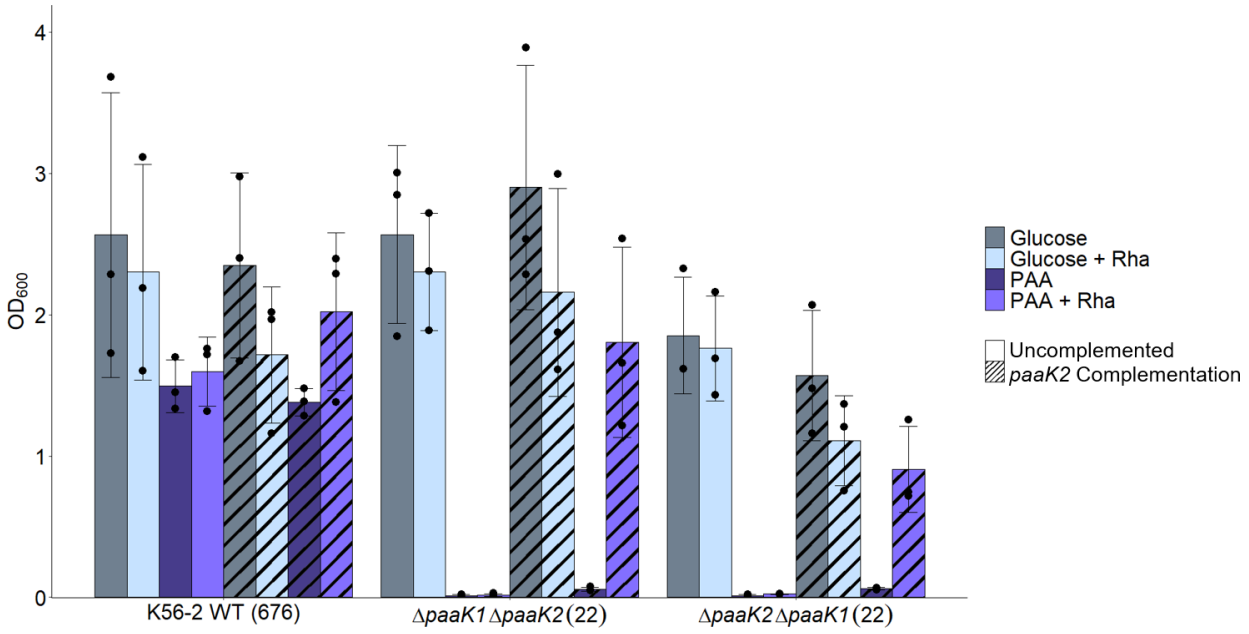


**Figure 14. *paaK2* complementation restores growth in PAA to Δ*paaK* deletion strains.**

Overnight cultures of *B. cenocepacia* K56-2 strains with and without *paaK2* complementation were washed twice in 1X PBS before being corrected to an $OD_{600}$ of 0.04. Strains were then grown in 1X M9 minimal media with 25 mM glucose or 5 mM phenylacetic acid (PAA) as a sole carbon source. 0.01% rhamnose (Rha) was added to induce expression of the *paaK2* gene. Optical density readings were taken at 24 hrs. Uncomplemented strains (empty bars) contain the plasmid backbone, pSCrhaB2, without the *paaK2* gene present, while *paaK2* complemented strains (striped bars) contain pKF2. Error bars are standard deviation of 3 biological replicates performed in triplicate, data points represent the average of each biological replicate.

Since *paaK2* complementation is sufficient to restore *paaK* ligase activity to the Δ*paaK1*Δ*paaK2*(22) and Δ*paaK2*Δ*paaK1*(22) strains, I tested the complemented strains on the exoprotease assay with PAA. I included PAA in the media because it is the only condition where I observed a significant decrease in the exoprotease activity of the Δ*paaK1*Δ*paaK2*(22) and Δ*paaK2*Δ*paaK1*(22) strains compared to the WT K56-2 (676) strain.

Presence of the pKF2 plasmid resulted in an increase in the exoprotease activity of the Δ*paaK1*Δ*paaK2*(22) and Δ*paaK2*Δ*paaK1*(22) strains (Figure 15). However, this increase was more prevalent in the absence of rhamnose when the *paaK2* gene is not expected to be expressed. This could be due to the rhamnose system being leaky, which would result in the *paaK2* gene being expressed from pKF2 even in the absence of rhamnose. In addition, there was a decrease in the exoprotease activity in all strains, complemented and uncomplemented, due to the addition of rhamnose, however this was only significant in the *paaK2* complemented WT K56-2 (676) strain ($p<0.05$).

The *paaK2* complemented Δ*paaK1*Δ*paaK2*(22) and Δ*paaK2*Δ*paaK1*(22) strains in the presence of rhamnose are not significantly different from the *paaK2* complemented WT K56-2 (676) strain in the presence of rhamnose ($p>0.05$) (Figure 15). This suggests that complementation can restore exoprotease activity in PAA to the Δ*paaK1*Δ*paaK2*(22) and Δ*paaK2*Δ*paaK1*(22) strains. Additionally, both strains have significantly higher levels of exoprotease activity when complemented with *paaK2* compared to uncomplemented when in the presence of rhamnose ($p<0.05$). Overall, these results indicate that the reduction in exoprotease activity in the presence of PAA of the Δ*paaK1*Δ*paaK2*(22) and Δ*paaK2*Δ*paaK1*(22) strains is due to the deletion of *paaK* and not some other acquired mutation.

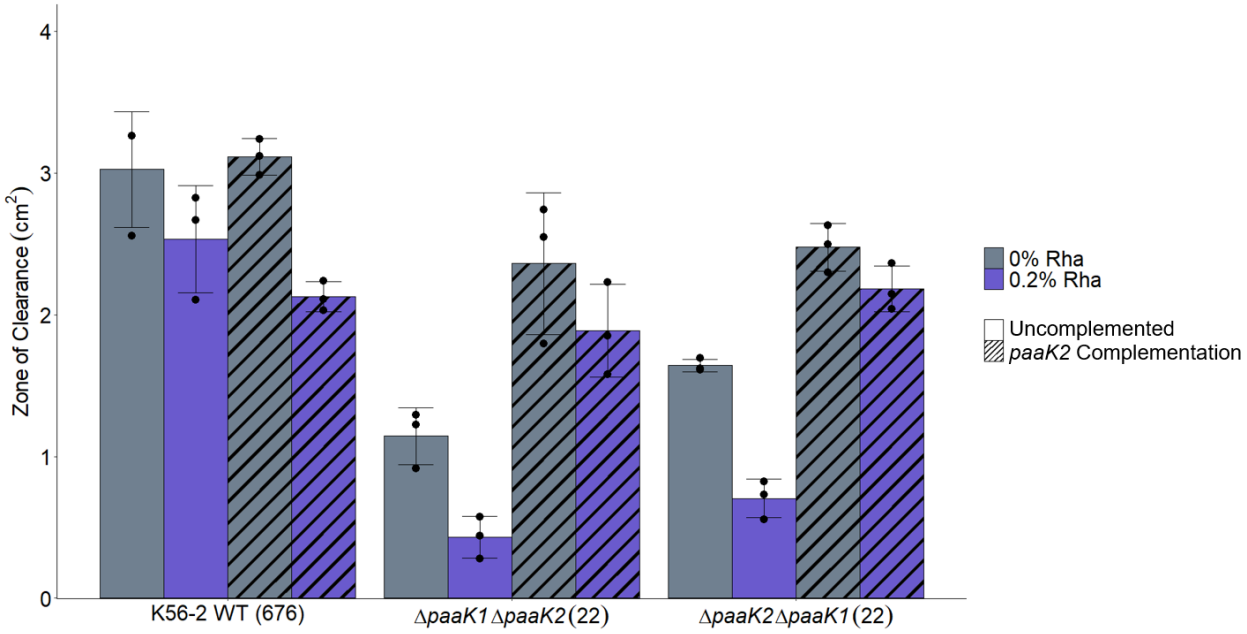


**Figure 15. Complementation with *paaK2* restores exoprotease activity in PAA to Δ*paaK* deletion strains.**

The exoprotease activity of *B. cenocepacia* strains with or without *paaK2* complementation was quantified by measuring the zone of clearance (excluding colonies) on agar plates containing 2% skim milk and 2 mM phenylacetic acid with or without the addition of 0.2% rhamnose (Rha) after a 48-hour incubation at 37°C. Rhamnose was added to plates to induce expression of the *paaK2* gene. Uncomplemented strains (empty bars) contain the plasmid backbone, pSCrhaB2, without the *paaK2* gene present, while *paaK2* complemented strains (striped bars) contain pKF2. Error bars are standard deviation of three biological replicates performed in duplicate, data points represent the average of each biological replicate.

*4.1.3 Untargeted Metabolomics was unable to reveal phenylalanine metabolism in ΔpaaK*

To investigate the differences between the Δ*paaABCDE* and Δ*paaK*(22) strains I ran an untargeted metabolomics experiment with the WT K56-2 (676), Δ*paaABCDE*, and Δ*paaK1*Δ*paaK2*(22) strains. Each strain was grown in M9 + 25 mM glycerol and with or without 2 mM $^{13}$C-labeled phenylalanine, or 2 mM PAA. This experiment aimed to determine how phenylalanine is metabolized differentially in the Δ*paaABCDE* and Δ*paaK1*Δ*paaK2*(22) strains. Additionally, insights into the differential levels of metabolites between the three strains may give an indication of the differences in pathogenicity between the strains in the different conditions tested. The WT K56-2 (676) strain and growth in M9 + 25 mM glycerol alone were both included as controls. All the samples were run through two different columns, HILIC and C18, which are optimized to detect different compounds and were treated as two separate data sets. Results obtained from Biozone Mass Spectrometry Facility at the University of Toronto were first filtered to find compounds that were present at significantly higher concentrations than the media blanks. Filtered compounds were then corrected to the internal standard, 4-chlorobenzoic acid, and the fold-change between different conditions and strains was calculated for each compound. A fold-change of ±2 was designated as a cutoff value for significance.

From the analysis, it was found that 213 compounds were identified to be present at significantly higher amounts than the media blanks using the HILIC column, and 108 compounds were identified with the C18 column. From the compounds identified with the HILIC column, 42 were found to be differentially present in the Δ*paaK1*Δ*paaK2*(22) strain between the phenylalanine and PAA conditions, while only 13 were identified with the C18 column. These results indicate that the metabolism of phenylalanine and PAA result in the differential production of metabolites in the Δ*paaK1*Δ*paaK2*(22) strain. Between the Δ*paaABCDE* and

Δ*paaK1*Δ*paaK2*(22) strains in phenylalanine, 44 compounds were found to be differentially present, and only 22 compounds were found to be differentially present between the two strains when grown in PAA from the HILIC column dataset. Seven of these compounds were found to be similar between the two conditions. With the C18 column dataset, 22 compounds were found to be differentially present between the Δ*paaABCDE* and Δ*paaK1*Δ*paaK2*(22) strain when grown in phenylalanine, and 12 compounds were identified to be differentially present when the strains were grown in PAA. Of these compounds, six were found to be similar. These results show that there is a larger difference in the metabolism of the two mutants when they are grown in phenylalanine compared to growth in PAA. This could indicate a differential metabolism for phenylalanine in the Δ*paaABCDE* and Δ*paaK1*Δ*paaK2*(22) strains.

Further analysis revealed that only 163 compounds were identified by a common name, while some compounds could not be identified by the software potentially due to the inclusion of uncommon elements. From these 163 compounds, 115 were recognized by MetaboAnalyst 5.0 when entered into the pathway analysis with compound names using the pathway library of *Pseudomonas putida* KT2440 (KEGG). Only 2 compounds were identified in the phenylalanine degradation pathway: phenylalanine and tyrosine. Unfortunately, there were no Co-A compounds identified in the metabolomics results which could be due to the difficulty in measuring these compounds. Co-A thioesters are instable metabolites due to their degradation in acidic environments, reactions with other thiol groups, and cleavage of the thioester bond which results in a difficulty of accurately identifying and measuring the concentrations of these compounds (Gil et al., 2015). Since the entirety of the PAA-CoA degradation pathway intermediates contain a Co-A, this may explain why none of these molecules were identified. However, I also did not identify any compounds involved in the homogentisate pathway which would be expected if phenylalanine

is being degraded through conversion to tyrosine. The $^{13}$C-labeled phenylalanine data does not appear to lend any further elucidation to the progression of phenylalanine degradation in the *B. cenocepacia* mutant strains as still no compound was identified in the phenylalanine degradation pathways. Further analysis on the metabolomics data and compounds identified is being completed.

### 4.2 Discussion

The involvement of the PAA degradation pathway in the pathogenicity of *B. cenocepacia* K56-2 is a misunderstood topic. It has been shown that this pathway is upregulated during *B. cenocepacia* infection in the CF lung, however, it is not known how it is involved in regulation of pathogenicity (Hamlin et al., 2009; Yoder-Himes et al., 2009). The presence of phenylalanine in the CF lung sputum (Barth & Pitt, 1996; Palmer et al., 2007) may explain the upregulation of the PAA degradation pathway during infection, however, it is also upregulated in the presence of certain antibiotics (Sass et al., 2011) indicating that it may play a larger role in *B. cenocepacia* survival. Previously in the Cardona lab, it was found that disruptions in the earlier steps of the pathway involving the *paaABCDE* operon results in an attenuation of pathogenicity (Law et al., 2008; Pribytkova et al., 2014). But disrupting the previous step of the pathway did not similarly result in an attenuation of pathogenicity (Lightly et al., 2019). These two results led to the hypothesis that PAA-CoA, the product of the first step in the pathway, played a role in CepIR regulated QS (Lightly et al., 2019), however in Chapter 3 I disproved a link between PAA-CoA and CepIR regulated QS. Additionally, remaking the Δ*paaK* mutants resulted in no difference from the WT K56-2 (676) strain regarding exoprotease activity or pathogenicity unless PAA was exogenously added to the media. This exogenously added PAA caused a decrease in exoprotease

activity and virulence in the new Δ*paaK1*Δ*paaK2*(22) and Δ*paaK2*Δ*paaK1*(22) strains. It was also found that the Δ*paaABCDE* strain is unable to grow in phenylalanine or PAA as a sole carbon source, and that addition of either compound results in a severe attenuation of exoprotease activity and virulence in this strain. These results are summarized in Table 4, which distinctly displays the differences in phenotypes between the addition of phenylalanine or PAA in the two mutants.

The Δ*paaABCDE* mutant can produce PAA-CoA while the Δ*paaK1*Δ*paaK2*(22) and Δ*paaK2*Δ*paaK1*(22) mutants are unable to produce PAA-CoA which may explain the differences in growth of these strains as PAA-CoA is a positive regulator of the PAA degradation pathway (Yudistira et al., 2011). However, the differences in the Δ*paaABCDE* and Δ*paaK* strains do not appear to be solely due to the presence of PAA-CoA, as the addition of PAA to the Δ*paaK* strains results in attenuation. This suggests that PAA and PAA-CoA both have a role in regulation of virulence in *B. cenocepacia*.

The untargeted metabolomics experiment found significant differences in the presence of metabolites in the Δ*paaK1*Δ*paaK2*(22) strain when grown in phenylalanine and PAA. This suggests that there are differences present in this strain when grown in the different carbon sources which could be resulting in the difference in phenotypes seen. However, I was unable to find a link between the compounds identified and phenylalanine metabolism or pathogenicity. Additionally, there was a higher number of differentially present metabolites between the Δ*paaABCDE* and Δ*paaK1*Δ*paaK2*(22) strain grown in phenylalanine than in PAA. This may be indicating a difference in metabolism for phenylalanine in the two strains, however the compounds identified are not in either phenylalanine degradation pathway discussed. The differential presence of metabolites in the Δ*paaABCDE* and Δ*paaK1*Δ*paaK2*(22) strains in the presence of PAA may further explain the differences in exoprotease activity and pathogenicity of these two strains when

in the presence of PAA. However, many of these compounds were not able to be identified in the analysis, thus further research is required. Additionally, it is unclear how the Δ*paaK* mutants can utilize phenylalanine without a functioning PAA degradation pathway.

**Table 4. Comparison of *B. cenocepacia* K56-2 PAA degradation mutants in phenylalanine and phenylacetic acid.**

| Test | Phe vs PAA | WT K56-2 (676) (%) | Δ*paaK1*Δ*paaK2*(22) (%) | Δ*paaABCDE* (%) |
|---|---|---|---|---|
| Growth (24 hrs)[a] | Glucose | 100 | 95 (±2) | 185 (±12) |
| | Phe | 127 (±27) | 103 (±26) | 1 (±0.4) |
| | PAA | 114 (±8) | 0.8 (±0.1) | 0.4 (±0.3) |
| Exoprotease Activity[b] | Control | 100 | 105 (±1) | 83 (±4) |
| | Phe | 134 (±1) | 132 (±3) | 0 (±0) |
| | PAA | 86 (±18) | 36 (±4) | 0 (±0) |
| *C. elegans* Killing (day 3)[c] | Control | 96 (±3) | 96 (±3) | 16 (±6) |
| | Phe | 96 (±1) | 91 (±1) | 7 (±5) |
| | PAA | 93 (±4) | 50 (±8) | 4 (±2) |
| *C. elegans* Killing (day 4)[c] | Control | 99 (±0.7) | 99 (±1) | 48 (±7) |
| | Phe | 100 (±0) | 98 (±1) | 10 (±7) |
| | PAA | 100 (±0) | 83 (±6) | 6 (±2) |

[a]Growth is compared back to the WT K56-2 (676) strain in glucose

[b]Exoprotease activity is compared back to the WT K56-2 (676) strain without supplementation

[c]Values represent *C. elegans* percent mortality

## CHAPTER 5: CONCLUSIONS

The involvement of the phenylacetic acid degradation pathway in the virulence of *B. cenocepacia* K56-2 has been a long-studied phenomenon but is still not fully understood. Previous research showed that the *paaABCDE* operon is required for full virulence of *B. cenocepacia* in a *C. elegans* host model (Pribytkova et al., 2014). However, it was unclear whether PAA or PAA-CoA was causing the attenuation of virulence in this strain. The creation of a double *paaK* deletion strain, the previous step in the PAA degradation pathway, indicated that it was the result of PAA-CoA as it was found that this strain had increased virulence compared to the WT K56-2 strain in which it was made (Lightly et al., 2019). Further investigation into the increased virulence in this strain indicated a role for quorum sensing that was reliant on the absence of PAA-CoA (Lightly et al., 2019). However, as I found there is likely some other explanation for the increased virulence of the double *paaK* deletion strain as a newly created strain did not show the same increase in virulence. Furthermore, deleting the *paaK* ligase genes was insufficient to restore pathogenicity or virulence to a *cepR* deletion mutant. Overall, I demonstrated that PAA-CoA is not involved in CepIR QS regulated virulence in the *B. cenocepacia* K56-2 strain as previously hypothesized.

Creation of new double *paaK* deletion strains revealed that they had similar pathogenicity and exoprotease phenotypes to the WT K56-2 strain they were made in, except when PAA was included in the media. The inclusion of PAA resulted in a decrease in exoprotease activity and pathogenicity in a *C. elegans* host model. This indicated a role for PAA in the regulation of virulence in *B. cenocepacia*. However, the Δ*paaABCDE* strain has abolished exoprotease activity on plates containing phenylalanine or PAA and significantly reduced pathogenicity in a *C. elegans* host model in the presence of phenylalanine or PAA. These results indicate a significant role for PAA-CoA in the regulation of virulence in *B. cenocepacia* K56-2. Additionally, the double *paaK*

deletion mutant was able to grow on phenylalanine as a sole carbon source even with a disrupted PAA degradation pathway indicating that there may be another pathway for the degradation of phenylalanine in *B. cenocepacia* K56-2. I hypothesize that this alternative pathway is not activated in the Δ*paaABCDE* strain due to the buildup of PAA-CoA which has previously been shown as an activator of the PAA degradation pathway (Yudistira et al., 2011). Unfortunately, an untargeted metabolomics experiment was unsuccessful in identifying the alternative pathway that could be responsible for the degradation of phenylalanine in the Δ*paaK1*Δ*paaK2*(22) strain.

Future directions of this research could include investigation into the degradation of phenylalanine in the Δ*paaABCDE* and Δ*paaK* strains to elucidate the differential growth present in these two strains. This could potentially be done through a transposon sequencing (Tn-Seq) experiment to identify genes that when interrupted result in the mutant strains losing the ability to grow on phenylalanine as a sole carbon source. This experiment could be done with transposon mutagenesis and subsequent sequencing of the insertion sites (Tn-Seq circle) which has previously been used in the Cardona lab (Gislason et al., 2017). Transposon mutagenesis could be done in the WT K56-2 (676), Δ*paaABCDE*, and Δ*paaK1*Δ*paaK2*(22) strains. This would allow the identification of genes that when interrupted result in the different strains' loss of the ability to use phenylalanine as a sole carbon source. It would be important to include the WT K56-2 (676) strain and Δ*paaABCDE* strain to filter potential genes that when interrupted result in loss of growth due to other confounding factors. The transposon mutants would be plated first on LB and then plated on M9 minimal media with phenylalanine as a sole carbon source. Mutants that cannot grow on phenylalanine would be selected from the LB plates and sequenced to determine which gene is interrupted in this strain. From this analysis it would be able to be determined if there is a secondary phenylalanine degradation pathway that is present in the Δ*paaK1*Δ*paaK2*(22) strain that is not

active in the Δ*paaABCDE* strain. A similar experiment was performed to identify the genes required for the metabolism of aromatic compounds in *Pseudomonas putida* U by Arias-Barrau et al., 2004, which was able to identify three mutant strains that were unable to use phenylalanine or tyrosine as sole carbon or energy sources. Subsequent analysis done in this strain revealed that disruption of the homogentisate pathway in these transposon insertion mutants was responsible for the loss of growth on phenylalanine or tyrosine (Arias-Barrau et al., 2004). Completing a similar Tn-Seq experiment in *B. cenocepacia* WT and mutant strains would be useful in further understanding the degradation of phenylalanine in *B. cenocepacia* K56-2. This knowledge would be useful since it has been previously shown that phenylalanine is present in the sputum of CF patients (Barth & Pitt, 1996; Palmer et al., 2007).

Further research is also required to investigate the differential virulence phenotypes of the Δ*paaABCDE* and Δ*paaK* mutants when in the presence of phenylalanine and PAA. An RNA-Seq experiment may be useful in identifying genes that are differentially expressed in these two mutants compared to the WT K56-2 (676) strain and in the presence of phenylalanine or PAA. This experiment may identify alternative genes that play a role in regulating virulence in *B. cenocepacia.* Prior research has shown that *B. cenocepacia* has multiple different genes that may play a role in the regulation of virulence through the QS system. Previously it was found that *B. cenocepacia* can undergo a colony morphology change to a shiny phenotype that is the result of either missing or reduced extracellular matrix (Bernier et al., 2007). These colonies were found to have attenuated virulence in an alfalfa infection model and it was discovered that a LysR-type regulator gene was disrupted in these strains (Bernier et al., 2007). Further investigation revealed that this regulator was ShvR which is positively regulated by CepR (O'Grady et al., 2011). Additionally it was found that ShvR negatively autoregulates itself while also reducing the

expression of the CepIR and CciIR QS systems (O'Grady et al., 2011). A separate LysR family transcriptional regulator, *Bcal3178,* is regulated by *cepR* and was found to regulate biofilm formation and exoprotease activity (Wang et al., 2021). The finding of two separate genes that aid in regulation of virulence of *B. cenocepacia* indicate that there could be unknown genes that also play a role in *B. cenocepacia* pathogenicity. It is possible that while PAA-CoA and PAA have not been found to have a direct role in CepIR QS regulated virulence, these compounds could play a role in the regulation of downstream genes regulated by a QS system present in *B. cenocepacia.* The interplay between metabolism and QS is also being investigated in different CF pathogens such as *S. aureus.* Stephens et al., 2022 investigated the interplay between metabolic regulators and quorum sensing in *S. aureus*. They found that disrupting metabolic transcriptional regulators also affected virulence factor production suggesting that virulence factors are not solely affected by QS but also by the energy state of the cells (Stephens et al., 2022). A similar mechanism may be present in *B. cenocepacia* which could lend some insight into the differential virulence phenotypes seen when the PAA degradation pathway is interrupted.

Investigation into the link between the PAA degradation pathway and pathogenicity in *B. cenocepacia* is an important topic. Understanding this link can better aid in our understanding of how bacteria cause infection and the important role of bacterial metabolism in a successful infection. This is even more important in *B. cenocepacia* due to the extremely harmful outcomes of infection with this bacterium for individuals living with cystic fibrosis. Further research is needed to fully understand the complicated mechanism of pathogenicity and how the interplay with phenylalanine and phenylacetic acid metabolism is involved.

## REFERENCES


Abisado, R. G., Benomar, S., Klaus, J. R., Dandekar, A. A., & Chandler, J. R. (2018). Bacterial Quorum Sensing and Microbial Community Interactions. *mBio*, *9*(3). https://doi.org/10.1128/mBio.02331-17

Alexander, B. D., Petzold, E. W., Reller, L. B., Palmer, S. M., Davis, R. D., Woods, C. W., & Lipuma, J. J. (2008). Survival after lung transplantation of cystic fibrosis patients infected with *Burkholderia cepacia* complex. *American Journal of Transplantation : Official Journal of the American Society of Transplantation and the American Society of Transplant Surgeons*, *8*(5), 1025–1030. https://doi.org/10.1111/j.1600-6143.2008.02186.x; 10.1111/j.1600-6143.2008.02186.x

Arias-Barrau, E., Olivera, E. R., Luengo, J. M., Fernandez, C., Galan, B., Garcia, J. L., Diaz, E., & Minambres, B. (2004). The homogentisate pathway: A central catabolic pathway involved in the degradation of L-phenylalanine, L-tyrosine, and 3-hydroxyphenylacetate in *Pseudomonas putida*. *Journal of Bacteriology*, *186*(15), 5062–5077. https://doi.org/10.1128/JB.186.15.5062-5077.2004 [doi]; 186/15/5062 [pii]

Aubert, D. F., Hamad, M. A., & Valvano, M. A. (2014). A markerless deletion method for genetic manipulation of *Burkholderia cenocepacia* and other multidrug-resistant gram-negative bacteria. *Methods in Molecular Biology (Clifton, N.J.)*, *1197*, 311–327. https://doi.org/10.1007/978-1-4939-1261-2_18

Aubert, D. F., O'Grady, E. P., Hamad, M. A., Sokol, P. A., & Valvano, M. A. (2013). The *Burkholderia cenocepacia* sensor kinase hybrid AtsR is a global regulator modulating quorum-sensing signalling. *Environmental Microbiology*, *15*(2), 372–385. https://doi.org/10.1111/j.1462-2920.2012.02828.x

Barth, A. L., & Pitt, T. L. (1996). The high amino-acid content of sputum from cystic fibrosis patients promotes growth of auxotrophic *Pseudomonas aeruginosa*. *Journal of Medical Microbiology*, *45*(2), 110–119. 1106.

Bassler, B. L. (1999). How bacteria talk to each other: Regulation of gene expression by quorum sensing. *Current Opinion in Microbiology*, *2*(6), 582–587.

Bernier, S. P., Nguyen, D. T., & Sokol, P. A. (2007). A LysR-Type Transcriptional Regulator in *Burkholderia cenocepacia* Influences Colony Morphology and Virulence. *Infection and Immunity*, *76*(1), 38–47. https://doi.org/10.1128/IAI.00874-07

Blanchard, A. C., & Waters, V. J. (2022). Opportunistic Pathogens in Cystic Fibrosis: Epidemiology and Pathogenesis of Lung Infection. *Journal of the Pediatric Infectious Diseases Society*, *11*(Supplement_2), S3–S12. https://doi.org/10.1093/jpids/piac052

Cardona, S. T., & Valvano, M. A. (2005). An expression vector containing a rhamnose-inducible promoter provides tightly regulated gene expression in *Burkholderia cenocepacia*. *Plasmid*, *54*(3), 219–228. 2. https://doi.org/10.1016/j.plasmid.2005.03.004

Coenye, T., & Vandamme, P. (2003). Diversity and significance of *Burkholderia* species occupying diverse ecological niches. *Environ.Microbiol.*, *5*(9), 719-729. 638.

Daccò, V., Alicandro, G., Consales, A., Rosazza, C., Sciarrabba, C. S., Cariani, L., & Colombo, C. (2023). Cepacia syndrome in cystic fibrosis: A systematic review of the literature and possible new perspectives in treatment. *Pediatric Pulmonology*, *58*(5), 1337–1343. https://doi.org/10.1002/ppul.26359

Darling, P., Chan, M., Cox, A. D., & Sokol, P. A. (1998). Siderophore production by cystic fibrosis isolates of *Burkholderia cepacia*. *Infection and Immunity*, *66*(2), 874–877.

Eberl, L., & Vandamme, P. (2016). Members of the genus *Burkholderia*: Good and bad guys. *F1000Research*, *5*, 1007. https://doi.org/10.12688/f1000research.8221.1

Figurski, D. H., & Helinski, D. R. (1979). Replication of an origin-containing derivative of plasmid RK2 dependent on a plasmid function provided in trans. *Proceedings of the National Academy of Sciences of the United States of America*, *76*(4), 1648–1652.

Flannagan, R. S., Linn, T., & Valvano, M. A. (2008). A system for the construction of targeted unmarked gene deletions in the genus *Burkholderia*. *Environmental Microbiology*, *10*(6), 1652–1660. https://doi.org/10.1111/j.1462-2920.2008.01576.x

Gil, A., Siegel, D., Permentier, H., Reijngoud, D.-J., Dekker, F., & Bischoff, R. (2015). Stability of energy metabolites—An often overlooked issue in metabolomics studies: A review. *ELECTROPHORESIS*, *36*(18), 2156–2169. https://doi.org/10.1002/elps.201500031

Gislason, A. S., Turner, K., Domaratzki, M., & Cardona, S. T. (2017). Comparative analysis of the *Burkholderia cenocepacia* K56-2 essential genome reveals cell envelope functions that are uniquely required for survival in species of the genus *Burkholderia*. *Microbial Genomics*, *3*(11), e000140. https://doi.org/10.1099/mgen.0.000140

Gotschlich, A., Huber, B., Geisenberger, O., Tögl, A., Steidle, A., Riedel, K., Hill, P., Tümmler, B., Vandamme, P., Middleton, B., Camara, M., Williams, P., Hardman, A., & Eberl, L. (2001). Synthesis of Multiple N-Acylhomoserine Lactones is Wide-spread Among the Members of the *Burkholderia cepacia* Complex. *Systematic and Applied Microbiology*, *24*(1), 1–14. https://doi.org/10.1078/0723-2020-00013

Hamlin, J. N., Bloodworth, R. A., & Cardona, S. T. (2009). Regulation of phenylacetic acid degradation genes of *Burkholderia cenocepacia* K56-2. *BMC Microbiology, 9*, 222. 14. https://doi.org/10.1186/1471-2180-9-222

Henry, D. A., Campbell, M. E., LiPuma, J. J., & Speert, D. P. (1997). Identification of *Burkholderia cepacia* isolates from patients with cystic fibrosis and use of a simple new selective medium. *Journal of Clinical Microbiology*, *35*(3), 614–619.

Herrera, M. C., Duque, E., Rodriguez-Herva, J. J., Fernandez-Escamilla, A. M., & Ramos, J. L. (2010). Identification and characterization of the PhhR regulon in *Pseudomonas putida*. *Environmental Microbiology*, *12*(6), 1427–1438. 1737. https://doi.org/10.1111/j.1462-2920.2009.02124.x

Herrera, M. C., & Ramos, J. L. (2007). Catabolism of phenylalanine by *Pseudomonas putida*: The NtrC-family PhhR regulator binds to two sites upstream from the *phhA* gene and stimulates transcription with sigma70. *Journal of Molecular Biology*, *366*(5), 1374–1386. https://doi.org/S0022-2836(06)01667-6 [pii]; 10.1016/j.jmb.2006.12.008 [doi]

Hogan, A. M., Rahman, A. S. M. Z., Lightly, T. J., & Cardona, S. T. (2019). A broad-host-range CRISPRi toolkit for silencing gene expression in *Burkholderia*. *ACS Synthetic Biology*, *8*(10), 2372–2384. https://doi.org/10.1021/acssynbio.9b00232

Jiao, M., He, W., Ouyang, Z., Shi, Q., & Wen, Y. (2022). Progress in structural and functional study of the bacterial phenylacetic acid catabolic pathway, its role in pathogenicity and antibiotic resistance. *Frontiers in Microbiology*, *13*, 964019. https://doi.org/10.3389/fmicb.2022.964019

Kanehisa, M. (2019). Toward understanding the origin and evolution of cellular organisms. *Protein Science : A Publication of the Protein Society*, *28*(11), 1947–1951. https://doi.org/10.1002/pro.3715

Kanehisa, M., Furumichi, M., Sato, Y., Kawashima, M., & Ishiguro-Watanabe, M. (2022). KEGG for taxonomy-based analysis of pathways and genomes. *Nucleic Acids Research*, *51*(D1), D587–D592. https://doi.org/10.1093/nar/gkac963

Kanehisa, M., & Goto, S. (2000). KEGG: Kyoto Encyclopedia of Genes and Genomes. *Nucleic Acids Research*, *28*(1), 27–30.

Kashyap, S., Sharma, P., & Capalash, N. (2021). Potential genes associated with survival of *Acinetobacter baumannii* under ciprofloxacin stress. *Microbes and Infection*, *23*(9), 104844. https://doi.org/10.1016/j.micinf.2021.104844

Kothe, M., Antl, M., Huber, B., Stoecker, K., Ebrecht, D., Steinmetz, I., & Eberl, L. (2003). Killing of *Caenorhabditis elegans* by *Burkholderia cepacia* is controlled by the *cep* quorum-sensing system. *Cellular Microbiology*, *5*(5), 343–351.

Law, R. J., Hamlin, J. N. R., Sivro, A., McCorrister, S. J., Cardama, G. A., & Cardona, S. T. (2008). A functional phenylacetic acid catabolic pathway is required for full pathogenicity of *Burkholderia cenocepacia* in the *Caenorhabditis elegans* host model. *J. Bacteriol.*, *190*(21), 7209–7218. 3. https://doi.org/10.1128/JB.00481-08

Lewenza, S., Conway, B., Greenberg, E. P., & Sokol, P. A. (1999). Quorum sensing in *Burkholderia cepacia*: Identification of the LuxRI homologs CepRI. *Journal of Bacteriology*, *181*(3), 748–756.

Lightly, T. J., Frejuk, K. L., Groleau, M.-C., Chiarelli, L. R., Ras, C., Buroni, S., Déziel, E., Sorensen, J. L., & Cardona, S. T. (2019). Phenylacetyl-CoA, not phenylacetic acid, attenuates CepIR-regulated virulence in *Burkholderia cenocepacia*. *Applied and Environmental Microbiology*, *85:e01594-19*. https://doi.org/10.1128/AEM.01594-19

Lobo, L. J., & Noone, P. G. (2014). Respiratory infections in patients with cystic fibrosis undergoing lung transplantation. *The Lancet Respiratory Medicine*, *2*(1), 73–82. https://doi.org/10.1016/S2213-2600(13)70162-0

Luengo, J. M., García, J. L., & Olivera, E. R. (2001). The phenylacetyl-CoA catabolon: A complex catabolic unit with broad biotechnological applications. *Molecular Microbiology*, *39*(6), 1434–1442. https://doi.org/10.1046/j.1365-2958.2001.02344.x

Mahenthiralingam, E., Coenye, T., Chung, J. W., Speert, D. P., Govan, J. R., Taylor, P., & Vandamme, P. (2000). Diagnostically and experimentally useful panel of strains from the *Burkholderia cepacia* complex. *Journal of Clinical Microbiology*, *38*(2), 910–913.

Mahenthiralingam, E., Urban, T. A., & Goldberg, J. B. (2005). The multifarious, multireplicon *Burkholderia cepacia* complex. *Nature Reviews Microbiology*, *3*(2), 144–156.

Malott, R. J., Baldwin, A., Mahenthiralingam, E., & Sokol, P. A. (2005). Characterization of the cciIR quorum-sensing system in *Burkholderia cenocepacia*. *Infection and Immunity*, *73*(8), 4982–4992. https://doi.org/10.1128/IAI.73.8.4982-4992.2005

O'Grady, E. P., Nguyen, D. T., Weisskopf, L., Eberl, L., & Sokol, P. A. (2011). The *Burkholderia cenocepacia* LysR-type transcriptional regulator ShvR influences expression of quorum-sensing, protease, type II secretion, and *afc* genes. *Journal of Bacteriology*, *193*(1), 163–176. https://doi.org/10.1128/JB.00852-10

Palmer, K. L., Aye, L. M., & Whiteley, M. (2007). Nutritional cues control *Pseudomonas aeruginosa* multi-cellular behavior in cystic fibrosis sputum. *Journal of Bacteriology*, *189*(22), 8079–8087. 1130. https://doi.org/10.1128/JB.01138-07

Papenfort, K., & Bassler, B. L. (2016). Quorum sensing signal-response systems in Gram-negative bacteria. *Nature Reviews. Microbiology*, *14*(9), 576–588. https://doi.org/10.1038/nrmicro.2016.89

Pribytkova, T., Lightly, T. J., Kumar, B., Bernier, S. P., Sorensen, J. L., Surette, M. G., & Cardona, S. T. (2014). The attenuated virulence of a *Burkholderia cenocepacia paaABCDE* mutant is due to inhibition of quorum sensing by release of phenylacetic acid. *Molecular Microbiology*, *94*(3), 522–536. 32. https://doi.org/10.1111/mmi.12771

Sass, A., Marchbank, A., Tullis, E., Lipuma, J. J., & Mahenthiralingam, E. (2011). Spontaneous and evolutionary changes in the antibiotic resistance of *Burkholderia cenocepacia* observed by global gene expression analysis. *BMC Genomics*, *12*, 373. https://doi.org/10.1186/1471-2164-12-373

Scoffone, V. C., Trespidi, G., Chiarelli, L. R., Barbieri, G., & Buroni, S. (2019). Quorum Sensing as Antivirulence Target in Cystic Fibrosis Pathogens. *International Journal of Molecular Sciences*, *20*(8). https://doi.org/10.3390/ijms20081838

Sobotková, L., Grafková, J., & Kyslík, P. (2002). Effect of phenylacetic acid on the growth and production of penicillin G acylase of recombinant and host strains derived from *Escherichia coli* W. *Enzyme and Microbial Technology*, *31*(7), 992–999. https://doi.org/10.1016/S0141-0229(02)00216-8

Sokol, P. A., Sajjan, U., Visser, M. B., Gingues, S., Forstner, J., & Kooi, C. (2003). The CepIR Quorum-Sensing System Contributes to the Virulence of *Burkholderia cenocepacia* Respiratory Infections. *Microbiology*, *149*(Pt 12), 3649–3658.

Stephens, A. C., Thurlow, L. R., & Richardson, A. R. (2022). Mechanisms Behind the Indirect Impact of Metabolic Regulators on Virulence Factor Production in *Staphylococcus aureus*. *Microbiology Spectrum*, *10*(4), e0206322. https://doi.org/10.1128/spectrum.02063-22

Teufel, R., Friedrich, T., & Fuchs, G. (2012). An oxygenase that forms and deoxygenates toxic epoxide. *Nature*, *483*(7389), 359–362. 2025. https://doi.org/10.1038/nature10862

Teufel, R., Mascaraque, V., Ismail, W., Voss, M., Perera, J., Eisenreich, W., Haehnel, W., & Fuchs, G. (2010). Bacterial phenylalanine and phenylacetate catabolic pathway revealed. *Proceedings of the National Academy of Sciences of the United States of America*, *107*(32), 14390–14395. 1750. https://doi.org/10.1073/pnas.1005399107

Thornton, C. S., & Parkins, M. D. (2023). Microbial Epidemiology of the Cystic Fibrosis Airways: Past, Present, and Future. *Seminars in Respiratory and Critical Care Medicine*, s-0042-1758732. https://doi.org/10.1055/s-0042-1758732

Valvano, M. A., Keith, K. E., & Cardona, S. T. (2005). Survival and persistence of opportunistic *Burkholderia species* in host cells. *Current Opinion in Microbiology*, *8*(1), 99–105. 4.

Vial, L., Chapalain, A., Groleau, M. C., & Deziel, E. (2011). The various lifestyles of the *Burkholderia cepacia* complex species: A tribute to adaptation. *Environmental Microbiology*, *13*(1), 1–12. https://doi.org/10.1111/j.1462-2920.2010.02343.x; 10.1111/j.1462-2920.2010.02343.x

Wang, K., Li, X., Yang, C., Song, S., Cui, C., Zhou, X., & Deng, Y. (2021). A LysR Family Transcriptional Regulator Modulates *Burkholderia cenocepacia* Biofilm Formation and Protease Production. *Applied and Environmental Microbiology*, *87*(12), e00202-21. https://doi.org/10.1128/AEM.00202-21

Yoder-Himes, D. R., Chain, P. S., Zhu, Y., Wurtzel, O., Rubin, E. M., Tiedje, J. M., & Sorek, R. (2009). Mapping the *Burkholderia cenocepacia* niche response via high-throughput sequencing. *Proceedings of the National Academy of Sciences of the United States of America*, *106*(10), 3976–3981. 1469. https://doi.org/10.1073/pnas.0813403106

Yudistira, H., McClarty, L., Bloodworth, R. A., Hammond, S. A., Butcher, H., Mark, B. L., & Cardona, S. T. (2011). Phenylalanine induces *Burkholderia cenocepacia* phenylacetic acid catabolism through degradation to phenylacetyl-CoA in synthetic cystic fibrosis sputum medium. *Microbial Pathogenesis*, *51*, 183–196. 6. https://doi.org/10.1016/j.micpath.2011.04.002